Chemical and Biological Hazard Prevention

Studies and Research Projects

REPORT **R-919**

Efficiency Evaluation of N95 FFRs under Cyclic and Constant Flows

Ali Bahloul
Fariborz Haghighat
Reza Mostofi
Alireza Mahdavi
Claude Ostiguy

irsst

The Institut de recherche Robert-Sauvé en santé et en sécurité du travail (IRSST), established in Québec since 1980, is a scientific research organization well-known for the quality of its work and the expertise of its personnel.

OUR RESEARCH is *working* for you !

Mission

To contribute, through research, to the prevention of industrial accidents and occupational diseases and to the rehabilitation of affected workers;

To disseminate knowledge and serve as a scientific reference centre and expert;

To provide the laboratory services and expertise required to support the public occupational health and safety network.

Funded by the Commission des normes, de l'équité, de la santé et de la sécurité du travail, the IRSST has a board of directors made up of an equal number of employer and worker representatives.

To find out more

Visit our Web site for complete up-to-date information about the IRSST. All our publications can be downloaded at no charge.
www.irsst.qc.ca

To obtain the latest information on the research carried out or funded by the IRSST, subscribe to *Prévention au travail,* the free magazine published jointly by the IRSST and the CNESST.
Subscription: *preventionautravail.com*

Legal Deposit
Bibliothèque et Archives nationales du Québec
2016
ISBN: 978-2-89631-871-1 (PDF)
ISSN: 0820-8395

IRSST – Communications and Knowledge Transfer Division
505 De Maisonneuve Blvd. West
Montréal, Québec
H3A 3C2
Phone: 514 288-1551
publications@irsst.qc.ca
www.irsst.qc.ca

Chemical and Biological Hazard Prevention

Studies and Research Projects

REPORT **R-919**

Efficiency Evaluation of N95 FFRs under Cyclic and Constant Flows

Ali Bahloul[1], Fariborz Haghighat[2], Reza Mostofi[2], Alireza Mahdavi[2], Claude Ostiguy[1]

Clic Research
www.irsst.qc.ca

A PDF version of this publication is available on the IRSST Web site.

This study was funded by the IRSST. The conclusions and recommendations are solely those of the authors.
This publication is a translation of the French original; only the original version (R-860) is authoritative.

PEER REVIEW

In compliance with IRSST policy, the research results published in this document have been peer-reviewed.

ACKNOWLEDGEMENTS

The authors would like to express their gratitude to the Institut de recherche Robert-Sauvé en santé et en sécurité du travail (IRSST). They also would like to acknowledge the contributions of Simon Demers, Pierre Drouin, Gilles Paradis and Yves Cloutier from IRSST for their valuable help in maintaining the experimental set-ups.

SUMMARY

Ultrafine particles (UFPs) (diameter of particles, D_p < 100 nm) can be found in many industrial workplaces, where their long-term inhalation could result in serious detrimental impacts on health. In some situations, engineering and administrative controls are insufficient to adequately protect the workers from inhaling UFPs. Individual respiratory protection is then required, and N95 filtering facepiece respirators (FFRs) are the most widely used by industrial and healthcare workers.

A previous study on the efficiency of the N95 filter using a constant flow and a polydispersed aerosol showed that the maximum particle penetration in these filters was obtained for a size of particles of less than 100 nm and that the penetration exceeded the threshold penetration of 5 % for air flows higher than 85 L/min. The present investigation evaluates N95 FFRs efficiency by using a cyclic flow rate more representative of human breathing.

The experimental set-up previously used to evaluate the efficiency of N95 FFRs under constant flows was adapted to the cyclic flow configuration. The first objective was to investigate the individual impact of breathing frequency and inhalation flow rate on the efficiency of N95 FFRs. The experiments were performed for two peak inhalation flows (PIFs) (135 and 360 L/min) and two breathing frequencies (24 and 42 breaths per minute (BPM)) for a total of four cyclic flows. The second objective was to compare the efficiency of N95 FFRs under cyclic flows with the ones under constant flows equal to the cyclic flow minute volume, mean inhalation flow (MIF) and PIF. Minute volume is defined as the average volume of inhaled air for one minute of breathing, while MIF is determined as the average volume of inhaled air per inhalation cycle. PIF is the maximum flow obtained in any inhalation cycle. The selected constant and cyclic flows (with equivalent MIFs) were in the range of 42 to 360 L/min. Finally, the impact of particle loading time on N95 FFRs efficiency was investigated under cyclic and constant flows for periods of up to six hours. A cyclic flow (with equivalent MIF rate of 170 L/min) and two constant flow rates of 85 and 170 L/min were selected. In all experiments, the filters were exposed to polydispersed NaCl particles ranging from 10 to 205.4 nm.

The results showed that an increase in both PIF and breathing frequency could potentially raise the particle penetration through N95 FFRs. However, the effect of PIF was observed to be much more important than the effect of the frequency. It was also shown that, among three constant flows equal to the cyclic flow PIF, MIF and minute volume, a constant flow equal to MIF can much better predict the initial penetration of N95 FFRs obtained under the cyclic flow.

Finally, particle loading had a significant impact on particle penetration through N95 FFRs, while the trend in penetration changes, in terms of loading time, highly depended on the levels of relative humidity (RH). With low RH, the protection level increased with particle loading on the filter. Penetration of smaller particles (usually <100 nm) significantly dropped following a filter long-term exposure, and a distinct shift in the most penetrating particle size (MPPS) towards larger particles was also observed. With high RH, on the other hand, a reverse trend was observed, since particle penetration was generally increased with the loading time. In addition, this investigation showed that, in terms of loading time, a constant flow (equal to the cyclic flow MIF) could not necessarily predict particle penetration during cyclic flows for long-term exposure of the filters.

TABLE OF CONTENTS

LIST OF TABLES

LIST OF FIGURES

LIST OF ABBREVIATIONS

Abbreviation	Description
ANOVA	Analysis of Variance
BPM	Breath per Minute
CFR	Code of Federal Regulations
CMD	Count Median Diameter
CPC	Condensation Particle Counter
DFM	Dust-Fume-Mist
DMA	Differential Mobility Analyzer
DM	Dust-Mist
DOP	Dioctyl Phthalate
EC	Electrostatic Classifier
FFR	Filtering Facepiece Respirator
GSD	Geometric Standard Deviation
HEPA	High-Efficiency Particulate Air
IPA	Iso-propyl-alcohol (Iso-propanol)
ISO/TS	International Standard Organization / Technical Specification
MIF	Mean Inhalation Flow
Kr	Krypton
MMD	Mass Median Diameter
MPPS	Most Penetrating Particle Size
NaCl	Sodium Chloride

NIOSH	National Institute for Occupational Safety and Health
NP	Nanoparticle
NT	Nanotechnology
PIF	Peak Inhalation Flow
PSL	Polystyrene Latex
RH	Relative Humidity
SMPS	Scanning Mobility Particle Sizer
UFP	Ultrafine Particle

LIST OF SYMBOLS

Symbol	Description
C	Concentration
D_p	Particle Size
P	Penetration
Fr	Breathing Frequency
X_{PIF}	Enhancement Fraction Value for Peak Inhalation Flow
X_{Fr}	Enhancement Fraction Value for Breathing Frequency

1 BACKGROUND

1.1 Overview

Ultrafine particles (UFP) are referred to particles which possess at least one aerodynamic size which is smaller than 100 nm. There are two major sources for generations of UFPs: natural and man-made. Sea sprays and natural fumes resulting from forest fires or volcano activities are common examples of natural sources of UFPs [1,2]. Welding fumes, diesel fumes, and aircraft exhaust contain man-made UFPs [3–5]. Compared to UFPs (which are usually undesired contaminants), there are other sources of nanometric particles (<100 nm) which are voluntarily produced. For instance, as a recently emerging research and application field, nanotechnology (NT) has led to an industrial revolution, by creating, producing and manufacturing a wide range of new generation materials with specific characteristics. Such a remarkable growth is consequently accompanied by the creation of new products and new markets, the handling of a rapidly increasing volume of nanoparticles (NP) and the potential of exposing an exponentially growing number of workers to these NPs. NP, by definition, is described as "*a nano-object with all three external dimensions in the size range from 1 to 100 nm*" [6,7]. Air cleaning sprays, laser ablation and surface coatings (spraying and deposition on the surface) are known as common sources of NPs [8].

The main concern associated with exposure to particles in the nanometer range is their potential toxicity leading to serious health impacts. Once inhaled, NPs can be deposited deeply into the alveolar section of the lungs, and partially translocated to secondary target organs [9–12]. Some NPs generate oxidative stress, inflammation, fibrosis and other physiological effects, which could initiate the development of different diseases [9–14]. Depending on specific studies, many metrics should be considered with the toxicity of NPs. The most important ones include: mass concentration, number concentration and surface area [15,16]. For example, some toxicity studies of the UFPs and NPs found a good correlation between the surface area and the biological effects [1,17,18], while others found a better correlation between the number of particles and the biological effects [19]. It has been shown that mass concentration is not well correlated to the observed biological effects for nanometric particles. Oberdörster *et al.* and Donaldson *et al.* indicated that, for two samples of 250 nm and 20 nm particles having the same mass concentration (10 µg/cm^3), the number concentrations were 1 200 and 2 400 000 #/cm^3, respectively [20,21]. Oberdörster *et al.* also reported that animals exposed by inhalation to the same mass of 20 and 250 nm TiO_2 particles, both with an aerodynamic size of 250 nm (agglomerated 20 nm NPs), showed a higher lung irritation and translocation, and a lower lung clearance with the 20 nm NPs compared to the 250 nm particle sizes [22]. In this specific study, the relative toxicity was well correlated to the specific surface area of each sample. Therefore, a typical sample of UFPs or NPs is expected to have potentially more adverse health effects compared with larger particle samples with the same mass.

Epidemiological studies have indicated that exposure to UFPs with sizes less than 100 nm could result in severe respiratory and cardiovascular health effects [23,24]. Nonetheless, epidemiological studies are currently available only for UFPs because exposure of workers to NP is recent; no long-term exposure data are available yet. Therefore, an epidemiological data

regarding the health effects of NPs are extremely limited and further investigations are required [25].

Workers are exposed to UFPs and NPs in different work environments such as production, manufacturing, use and disposal of products [2,26]. In such cases, the possible exposure routes are normally inhalation, eye contact, skin adsorption and dermal penetrations [1]. Among these routes, inhalation is considered as the most significant exposure routes in most situations [27]. Available strategies such as engineering (enclosure, local exhaust ventilation, fume hoods, etc.) and administrative (exposure reduction time, work organization, etc.) controls are normally applied to control UFPs and NPs exposure. However, these strategies are not always sufficient to provide the workers with an acceptable level of exposure. In these specific situations, the inhalation of harmful UFPs and NPs can be controlled by means of filtering facepiece respirators (FFR), generally in conjunction with other control strategies. These respirators are broadly employed by industrial and health-care workers. These filters are generally inexpensive, available and comfortable [8,28], but should be used in last resort when the other control measures are insufficient to adequately protect the worker.

The National Institute for Occupational Safety and Health (NIOSH) has presented three classes of filter materials, each with three different levels of protection. These classes were N, R and P which were respectively referred as “non-resistant”, “resistant” and “proof” in terms of resistance against degradation by oil particles [29]. The protection levels were also 95, 99 and 100 which indicated a minimal particle removal efficiency of 95, 99 and 99.97 %, respectively. Based on the protection efficiency level (95, 99 or 99.97 %) each class of N, R or P could be suffixed by 95, 99 or 100. NIOSH-certified filters (N, R and P classes) are classified to support the regulations of the 42 Code of Federal Regulations, Part 84 (42 CFR 84) which was replaced to modify the 30 Code of Federal Regulations, Part 11 (30 CFR 11), 1995 [30]. Following the 42 CFR 84 (subpart 181) and NIOSH regulations, N-class filters should be exposed to NaCl challenge concentration with a count median diameter (CMD) of 75 nm and a maximum geometric standard deviation (GSD) of 1.86. P- and R-class filters must also be exposed to dioctyl phthalate (DOP) aerosols with a CMD of 165 nm and a maximum GSD of 1.6. Particles should be electrically neutralized to reflect the worst-case scenario. To obtain certifications by NIOSH and 42 CFR 84, filters are exposed to a constant air flow of 85 L/min (or 42.5 L/min if a dual-filter is evaluated). Particle penetration, calculated as the ratio of the aerosol concentration downstream to the aerosol concentration upstream at a mass diameter of 300 nm, measured with photometric light scattering methods, should be less than 5, 1 and 0.03 % for levels of 95, 99 and 100, respectively. The certifications mentioned above address particle penetration through material media itself, while fit testing is intended to address leakage issues.

There are two potential limitations associated with the certifications of NIOSH and 42 CFR 84 for the utilization of the FFRs. First, NIOSH tests the filtration efficiencies at about 300 nm, as this value represents the most penetrating particle size (MPPS) for mechanical filters. However, most FFRs are electrically charged, and various studies have shown the effect of electrostatic attraction of the charged media of the NIOSH-certified filters which dramatically shifts the MPPS towards nanometer size (<100 nm) [31–34]. The second limitation is related to the use of a constant flow (85 L/min). This approach may not fully represent the breathing flow since actual breathing is better represented by a cyclic pattern. Thus, it is necessary to investigate the efficiency of NIOSH-certified filters under cyclic flow and to compare the results with the ones

obtained when using a constant flow.

1.2 Particulate Filtration: Theoretical Approach

The use of FFRs is, in fact, based on the particulate filtration process to remove harmful particles from the inhaled air. The capability of filter material to efficiently capture the exposed particles depends on several factors varying with the physical and chemical properties of the filtering material (i.e. filter chemical composition, filter thickness, fiber packing density, charge of media, etc.), and the external exposure conditions (i.e. particle chemical composition, particle size, face velocity or airflow, steady or unsteady pattern of flow, charge of particles, temperature, relative humidity (RH), loading time, etc.). These external conditions could result in minor or substantial impact on the efficiency of individual filtration mechanisms as well as on the filter overall efficiency. The filter overall efficiency is estimated by combining the impact of individual filtration mechanisms efficiency. Hence, as a first step, it is useful to summarize the role of individual particulate filtration mechanisms.

1.2.1 Filtration Mechanisms

The particulate filtration is accomplished through four mechanisms [35]. Figure 1.1 provides the schematic approach for each filtration mechanism. These mechanisms are:

1- Inertial impaction;
2- Interception;
3- Diffusion; and
4- Electrostatic attraction.

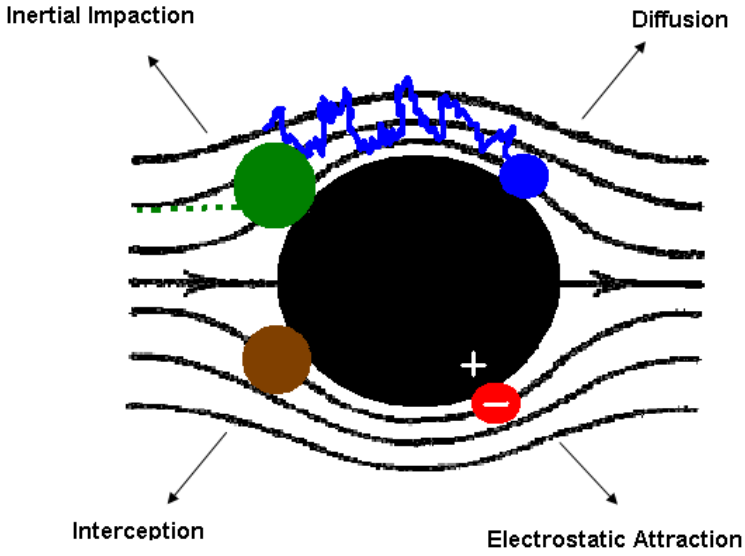

Figure 1.1 – Particulate filtration mechanisms (Adapted from Haghighat et al. [36]) *Inertial impaction* takes place when the particle inertia is too high to follow the changing direction of the airflow stream. The particle then impacts on the membrane of the filter [35]. Overall, the

particles which are approximately 1 μm or larger are effectively captured by this mechanism, which is negligible when dealing with nanometer size particles [37].

Interception takes place when a particle pursues its main streamline while coming within one particle radius from the surface of a fiber [35], and then making a contact between the particle and the filter media. Interception is not mainly influenced by the velocity of the particles, though it becomes more noticeable if particle size is increased [37]. The major difference between interception and inertial impaction is that no deviation from the main streamline takes place with interception, while deviation takes place for inertial impaction.

Diffusion, which is the predominant mechanism for capturing particles with sizes less than 0.2 μm, occurs because of the random Brownian motion of particles bouncing into the airflow and eventually hitting the filter media [37]. The irregular motion of particles, in fact, enhances the probability of a collision between particles and fiber in a non-intercepting streamline [35] which makes diffusion more significant rather than interception in capturing very small particles such as UFPs and NPs. As particle size is reduced, the diffusion becomes more pronounced due to the increased impact of Brownian motion. As the face velocity is reduced, particles go through the filter and the airflow moves more slowly. Consequently, the retention time is increased resulting in an increase in the rate of capture of the NPs through the diffusion mechanism.

The filtration devices removing particles by means of a combination of inertial impaction, interception and diffusion are referred as “mechanical filters” in the literature [27]. In order to increase the overall filter efficiency, an additional mechanism called *electrostatic attraction* can be added. This can be done by electrically charging either the media or the particles or both. Electrostatic attraction is reduced by increasing the face velocity. The charged filters showing electrostatic attraction in addition to other capturing mechanisms (diffusion, interception and inertial impaction) are referred as “electrostatic filters” [38–40]. Most of the commercially available NIOSH-approved N95 filters are known as electrostatic filters.

The overall filtration efficiency is obtained by combining the effect of all capturing mechanisms (impaction, interception, diffusion and electrostatic attraction). For sub-micrometer particles captured by mechanical filters, interception and diffusion are the most dominant mechanisms, while inertial impaction is negligible. A combination of the former mechanisms (diffusion and interception) leads to a minimal efficiency (i.e. a maximal particle penetration) at a certain particle size. This size is usually referred as the “Most Penetrating Particle Size (MPPS)” indicating the worst-case scenario at which the penetration reaches its highest value (figure 1.2). Based on the single fiber filtration theory, MPPS normally occurs at 300 nm for mechanical filters. For electrostatic filters, on the other hand, an additional mechanism, electrostatic attraction, combined with diffusion and interception, significantly raises the filtration efficiency and shifts the MPPS towards smaller sizes compared to mechanical filters.

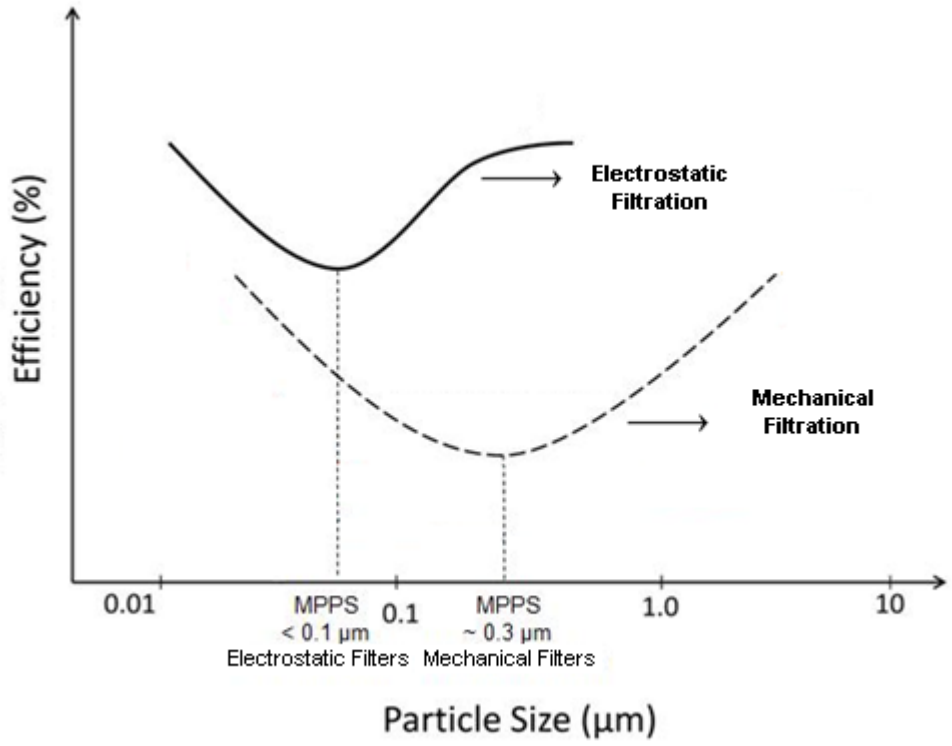

Figure 1.2 – Most penetrating particle size (MPPS) for mechanical and electrostatic filters

1.3 Particulate Filtration: Experimental Approach

From our literature review, the different factors contributing to the filtration efficiency and supported by experimental results are discussed in the following paragraphs.

1.3.1 Charge Effects

The impact of the electrostatic attraction mechanism in NIOSH-approved filters has been investigated in earlier studies [31,40,41]. The authors found that the efficiency of NIOSH-approved filters is dramatically reduced when the filters are dipped into isopropanol (IPA) to remove the electrostatic charges. For one model of N95, for instance, the penetration was increased from about 5 to 45 %, for "as-received" and "IPA-dipped" cases, respectively [31]. It was also observed that the MPPS for the IPA treated filters was substantially displaced towards larger sizes (from 50-100 nm to 250-350 nm). The latter findings were consistent with the particulate filtration theory due to change in the relative contribution of each filtration mechanism. Other investigations on other filter materials have also reported an increase in filtration efficiency for electrostatic filters compared to conventional filters [38,42–45].

In addition to the charge carried out by the filter media, the impact of the electrostatic attraction mechanism can also be influenced by the charges carried out by the particles, potentially resulting in lower particle penetrations (higher efficiency) [28,32,39,46–48]. Balazy *et al.*, for instance, measured the penetration of polydispersed NaCl particles (10-200 nm) through N95 respirators under 85 L/min airflow for two cases involving charged and neutralized particles

[32]. In this specific case, the charged particles were shown to have a higher collection (less penetration) compared with the neutralized particles. Such conclusion and other similar research findings suggest neutralizing the electrostatic charges on the particles in order to estimate the worst-case scenario for efficiency measurement.

1.3.2 Flow Effects

The impact of flow rate has been widely discussed [32-34,60,64] since higher flow rate is associated with higher workloads, which could potentially decrease the filtration efficiency. The discussion about the impact of flow rates covers both constant and cyclic flows. Constant flows are mostly selected in order to adapt the test criteria to the US Standard Method and Regulations (85 L/min according to 42 CFR 84, 1995). Cyclic flows, on the other hand, reflect the actual breathing flow in humans which follows a cyclic rather than a constant pattern. These items will be reviewed separately.

1.3.2.1 Impact of Constant Flow

Increasing flow rate (or face velocity) can significantly increase the particle penetration through filter media. Such penetration increase is mainly due to the reduction of the efficiency of the electrostatic and diffusion mechanisms [35,37]. Several studies have observed that an enhanced flow rate causes an increase in penetration (or a reduction in filtration efficiency) [8,28,32–34,41,43,44,47–56].

For example, Qian *et al.* measured the efficiency of the N95 and three conventional Dust-Mist (DM), Dust-Fume-Mist (DFM) and surgical masks under 32 and 85 L/min constant flow rates [44]. The tests were performed by generating monodispersed NaCl aerosols ranging from 0.1 to 0.6 µm and monodispersed polystyrene latex (PSL) ranging from 0.6 to 5.1 µm. They observed lower efficiency values for all filters under the constant flow rate of 85 L/min compared to the 32 L/min flow rate. Balazy *et al.* tested two N95 models under 30 and 85 L/min flow rates, exposed to polydispersed NaCl particles with a size ranging from 0.01 to 0.6 µm. They observed significantly higher particle penetrations for higher flow rates. Some test replicates, at higher air flow rate, exceeded the 5 % NIOSH threshold limit for N95 [32]. These authors also showed the same trend for bioaerosols such as MS2 viruses (size ranging from 10 to 80 nm) under the same flow rates (30 and 85 L/min) for N95 and surgical masks [43]. Huang *et al.* measured the effect of airflow rate on the IPA treated FFP1 (EN149:2001) fibrous filter under 30, 60 and 85 L/min using 4.5 nm to 10 µm NaCl aerosols and obtained similar results [41]. For example at 300 nm, particle penetrations for 30, 60 and 85 L/min flow rates were reported as 47, 66 and 79 %, respectively. Eninger *et al.* measured penetration of NaCl particles, MS2 viruses, *Bacillus subtilis* phage and T4 phage bioaerosols (polydispersed) through one model of N95 and two models of N99 respirators, for particle size ranging from 0.02 to 0.5 µm, with 30, 85 and 150 L/min flows [33]. Maximal penetration of NaCl particles was measured as 8.1, 4.8 and 1.4 % for 150, 85 and 30 L/min flows, respectively, for the N95 respirator. For the first model of N99, maximal penetration reached 10.2, 5.9 and 1.3 %, respectively; and for the second model of N99, these numbers were recorded as 6.6, 4.3 and 1 %, respectively [33]. The MPPS for all flow rates was found to fall between 30 and 70 nm with a slight tendency towards the smaller sizes at higher flow rates [33]. Mostofi *et al.* investigated the impact of increased flow rate (85, 135, 270 and 360 L/min) by exposing a model of N95 respirator to 15-200 nm polydispersed NaCl

particles [34]. Maximal penetration (at MPPS) reached 2.7, 6.6, 11.7 and 15.3 % for the tested flow rates, respectively. The MPPS was also observed to be displaced from 46 to 36 nm with the increasing flow rate (from 85 to 360 L/min) [34].

1.3.2.2 Impact of Cyclic Flow

The impact of cyclic flow rates on the particle penetration has also been studied [7,29,57–69]. Penetration levels between the cyclic and constant flows have particularly been addressed in a few studies with the objective to establish an appropriate correlation between the certification protocol and real workplace conditions. The initial penetrations under cyclic flows were typically compared with the penetrations measured under constant flows equal to the minute volume, mean inhalation flow (MIF) and peak inhalation flow (PIF) of the cyclic flows (figure 1.3). Minute volume is defined as the average amount of air inhaled per one minute of breathing, while MIF is characterized by the amount of total volume of air inhaled in one inhalation cycle divided by the inhalation cycle period. PIF is the maximum flow obtained in one inhalation cycle. For a sinusoidal flow (as selected for all cyclic flows in this study), regardless of the breathing frequency, the PIF is π times the minute volume and π /2 times the MIF (or the MIF is twice the minute volume).

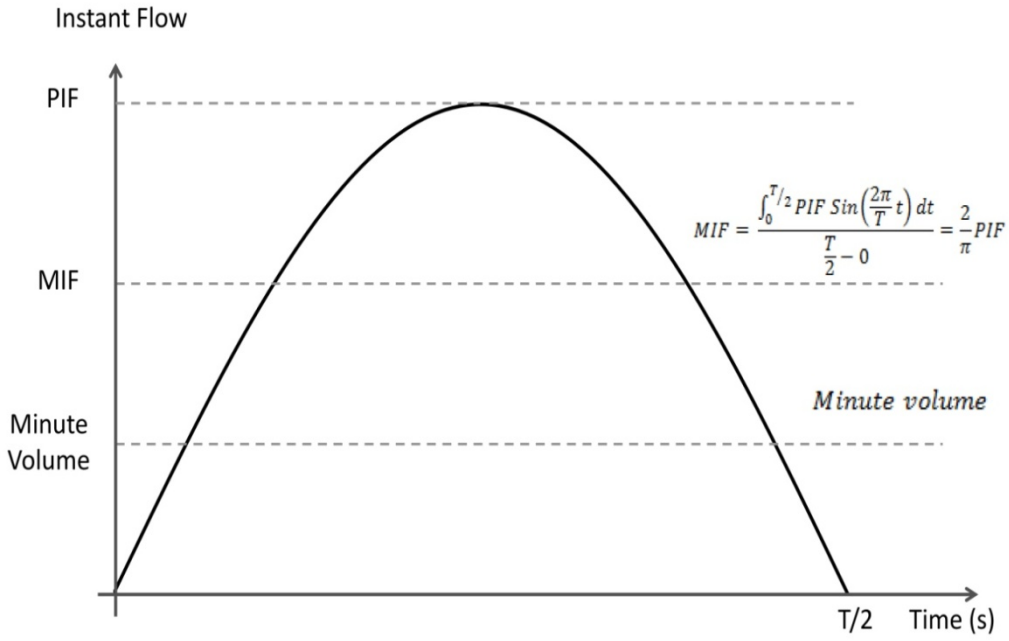

Figure 1.3 – Interrelation of cyclic flow and constant flows equal to cyclic flow; minute volume, mean inhalation flow (MIF) and peak inhalation flow (PIF); T/2 is half the respiration cycle period, representing here the inhalation cycle period only

Stafford *et al.* tested the efficiency of three models of respirator filter cartridges by comparing the impact of three cyclic flows with the MIFs of 30, 35 and 53 L/min and a constant flow of 32 L/min on the penetration of monodispersed PSL and DOP particles [58]. The PSL and DOP particle sizes selected were 0.176-2.02 μm and 0.3 μm, respectively. Brosseau *et al.* also

investigated the penetration of silica (0.46 μm) and asbestos (4.5 µm as length and 0.2 µm as width) particles on the DM filters under cyclic flows with equivalent PIF of 100 L/min and MIF of 76 L/min compared with constant flow rate of 32 L/min [59]. The results of both studies indicated that the penetration measured with the cyclic flow was typically higher than the penetration obtained by the equivalent constant flow [58,59].

More recently, additional studies tried to find a relationship between cyclic and equivalent constant flows for NIOSH-approved filters. Richardson *et al.* and Eshbaugh *et al.* [60,64] evaluated the efficiency of N95 and P100 FFRs and cartridges challenged by 0.02-2.7 nm particles. N-series filters were challenged by NaCl (0.02-0.3 µm) and PSL (0.7-2.9 µm), while P-series filters were challenged with DOP (0.02-0.3 µm) and polyalpha olefin oil (0.7-2.9 µm). Filters were tested under three constant flows with rates of 85, 270 and 360 L/min and cyclic flows with rates of 40, 85, 115 and 135 L/min as minute volume (or 135, 270, 360 and 430 L/min as PIF, respectively). It was concluded that a constant flow equal to the MIF or PIF of the cyclic flow could better predict the penetration under a cyclic flow [60,64]. Their results showed that penetration of cyclic flows with minute volume of 85 L/min (equal to 270 L/min as PIF) was higher when compared with the constant flow of 85 L/min. It was also indicated that the cyclic flows tended to cause a slight increase in penetration, when constant flows with rates of 85 and 270 L/min and cyclic flows with the same values as MIF were compared. Unlike minute volume and MIF, the penetration under constant flows of 270 and 360 L/min was higher than the cyclic flow with same values as PIF [60,64].

Haruta *et al.* assessed the effect of constant flows with rates of 15, 30, 85 and 135 L/min and cyclic flows with the equivalent MIFs. The tests were performed with PSL UFPs with effective sizes of 25, 65 and 99 nm (GSD <1.1; monodispersed) [61]. Consistent with the results of Richardson *et al.* [60], the magnitude of penetration was found to be higher with the cyclic flow than with the constant flow for the first two constant-cyclic couples (15 and 30 L/min). However, almost similar values were recorded for the penetration measured under constant and cyclic flows with a rate of 85 L/min. For the highest flow selection (135 L/min), the penetration under the constant flow was higher compared with penetrations measured with the cyclic flow [61].

Wang *et al.* compared the penetration of N95 and P95 dual-filter cartridges obtained by the constant flow ranging from 32 to 320 L/min and the cyclic flows with equivalent minute volumes ranging from 16 to 130 L/min when they were challenged with PSL particles (0.3 µm) [66]. Similar to the results of Richardson *et al.* and Eshbaugh *et al.* [60,64], the penetration obtained under cyclic flow was higher than penetrations measured with the constant flow equivalent to minute volume and MIF, but less than penetrations measured under constant flow with equivalent PIF. Rather than the comparison between constant and cyclic flow, they also measured the penetration of 0.3 μm PSL particles through N95 and P95 cartridges with dual-filter elastomeric half-face masks under various cyclic flows with the same equivalent minute ventilation (minute volume of the cyclic flow) of 50 L/min but different patterns, including two sinusoidal, one trapezoidal and one exponential flows. They observed higher penetration values with the exponential cyclic flow (which had higher PIF), almost the same values for the two sinusoidal flows (which had the same PIF but different frequencies and tidal volumes), and lower for the trapezoidal flow (which had the lowest PIF). Additionally, the constant minute volume flow led to the lowest penetration compared to all the selected cyclic flows.

In a recent study, Gardner *et al.* investigated the effect of constant and cyclic flows on the penetration of inert aerosol (NaCl, 50 nm) and MS2 viruses (500 nm as a Mass Median Diameter (MMD)) on N95 and P100 FFR and cartridges, for two constant flow rates (85 and 270 L/min) and two cyclic flow rates (85 and 135 L/min as minute volume) [69]. They found that all N95 and P100 filters efficiency met or exceeded the capturing efficiency for MS2 viruses for either low or high flow rates. The comparison between the constant and cyclic flow penetration also indicated that a constant flow equal to MIF or PIF of the cyclic flow would better represent the cyclic flow penetration.

Other recent studies have also investigated the impact of breathing frequency in cyclic flows on the efficiency of various respiratory protection devices [70-72]. In general, the effect of breathing frequency was more complex compared to other parameters such as flow rate. For instance, He *et al.* [70] measured the impact of breathing frequency for size-dependent (20-500 nm) particle penetration through a filter, with various flow rates (15 to 85 L/min as MIF) through N95 FFRs and surgical masks. Five frequency values were selected within 10 to 30 breaths per minute (BPM). The observations showed that the effect of breathing frequency on particle penetration was less considerable, especially at lower flow rates, while the impact of particle size and flow rate was more significant. Generally, for higher MIFs, particle penetration was high at low breathing frequencies (closer to 10 BPM). In another study, He *et al.* [71] tested the impact of breathing frequency (10 to 30 BPM) for the size-independent (20-500 nm) on particle penetration, through a filter for cyclic flows of 15 to 85 L/min (MIF). Their results indicated that both flow rate and breathing frequency have a significant impact on particle penetration through filters, despite the complexity of the breathing frequency effect.

1.3.3 Particle Loading Effect

In general, for mechanical filters, the loading effect results in an enhancement in filtration efficiency as well as an increase in pressure drop [77,78]. Leung and Hung [78] also observed that, the MPPS shifts towards smaller sizes, which according to the authors' explanation, was due to the agglomerated particles improving the capture efficiency by diffusion and interception mechanisms with a more prominent way via interception. For electrostatic filters, on the other hand, the penetration is firstly increased (capture efficiency is decreased), since electrostatic attraction forces are attenuated by deposited particles. Such an increase in penetration is then followed by a reverse trend (decrease in penetration) after a certain particle deposit, since the filter could behave like a mechanical filter [38,45,79].

Investigations of loading effect on NIOSH-approved filters have been, on the other hand, very limited [34,79,80]. Barrett and Rousseau tested advanced the electret filter media (materials prepared for NIOSH-approved filters: N, R and P series) with loading of NaCl (0.08 µm as CMD and 0.2 µm as MMD) and DOP (0.18 µm as CMD and 0.3 µm as MMD) under 85 L/min constant flow, up to 200 mg challenge aerosol load [79]. They found out that the penetration and pressure drop were initially increased with the aerosol challenge load. However, the loading penetration of advanced electrets filters was found to be 10 fold smaller than the loading penetrations obtained for conventional electrostatically charged blown microfiber media (with the same pressure drop for both filter materials). Moyer and Bergman determined the loading effect of small masses of NaCl (CMD of 75 nm with a GSD of less than 1.86) for a challenge concentration of typically 5 ± 1 mg/day on N95 filters, under 85 L/min constant flow rate [80].

The loading tests were performed for a period of one day and were repeated once a week for a period of weeks. Between two consecutive testing periods, the N95 filters were kept uncovered, outside the test laboratory, without exposure to NaCl particles. The results showed that, within a one-day period (in each single week), the particle penetrations were decreased with the loading time. However, between consecutive periods (from one week to the next week) an increase in the average penetration was observed. Mostofi *et al.* investigated the loading effect of polydispersed NaCl particles (ranging from 15 to 200 nm) on N95 FFRs for a period of 5 hours under a constant flow of 85 L/min [34]. The results indicated that a significant decrease in penetration occurred for particles with sizes less than 100 nm. The average penetration for nanometer sizes was, for instance, reduced from 1.76 to 0.87 % for the initial and final stage of loading, respectively. However, for larger particles the penetration slightly increased with the exposure time. The final average penetration for 100-200 nm was recorded as 1.07 % compared with an initial penetration of 0.71 %. The MPPS was also observed to be significantly shifted from 41 to 66 nm for initial and final stages, respectively.

As reported above, the results from previous studies give useful information regarding the efficiency of N95 filters under cyclic flows and the comparison with constant flows. Nonetheless, the information available in the literature is still limited. Unlike the constant flow, which is characterized by only one parameter (magnitude of flow), the cyclic flow is characterized by at least two parameters: breathing frequency and PIF. It is therefore not known which of these parameters is more influential. It should be considered that breathing frequency and inhalation flow rate simultaneously increase from sedentary to heavy workloads in a real respiratory process [73–76]. In such case, variations in penetration though respirator filters could be attributed to the rise in both flow and frequency. Hence, it is necessary to investigate the individual contribution of each parameter in cyclic flows. Caution should be applied in comparing results of previous studies as the experimental set-up used were different. For instance, some of the earlier studies ignored the exhalation cycles and only considered the inhalation portion [61,63,64,66] (sub-micrometer test apparatus in [64]); while other studies considered both inhalation and exhalation [7,62,65,67,69].

The difference is not only limited to the experimental set-up, but also there is no consensus in the literature when constant and cyclic flow filtration efficiency are compared. This could be due to the observed diversity in experimental set-ups, types of filter materials and types of challenge particles used. Moreover, the experiments comparing the efficiency of respirator filters, against inert particles, under constant and cyclic flows were mainly performed using monodispersed particles. No earlier study investigated this comparison for polydispersed inert particles. Polydispersed particles reflect a more realistic situation.

The effect of loading time for polydispersed particles on the efficiency of N95 filters has been less studied. Particularly, the impact of polydispersed particles in terms of loading time was discussed by only one previously peer-reviewed paper [34]. Nonetheless, the selection of this latter study was limited to only a single constant flow and a single RH. The loading time effect under cyclic flows as well as its comparison under constant flows is still unknown. It remains unclear what the case would be if the test conditions (ex. RH) were varying during the loading of the filter.

1.4 Objectives

The aim of the study is to evaluate the filtration efficiency of an N95 FFR model in conditions simulating workers' breathing and to compare the effect of constant and cyclic flows on the N95 filtration efficiency. The specific objectives are the followings:

- Adapt the experimental set-up used for constant flow testing so it can be used for cyclic flow rate testing;
- Develop a procedure and investigate the individual impact of breathing frequency and flow rate on the efficiency of one model of N95 FFR. The study is performed using two different experimental set-ups ("inhalation only" and "inhalation and exhalation") in order to explore the impact of the type of experimental set-up;
- Address the impact of polydispersed particle penetration (mostly ultrafine range <100 nm) under cyclic flows and compare it with the penetrations obtained under constant flows equivalent to the minute volume, MIF and PIF of the cyclic flow;
- Evaluate the efficiency of N95 filters under both constant and cyclic flows (with minute volume of 85 L/min) taking into account the initial penetration and the penetration associated with the loading time using various humidity conditions.

2 MATERIAL AND METHODS

2.1 Experimental Design

2.1.1 Set-up Configuration

The experimental set-up used in a previous study [36] for constant flow testing was adapted to a cyclic flow configuration to measure the efficiency of FFRs against UFPs (Figures 2.1 and 2.2). The set-up comprised an experimental chamber, a manikin head, a particle generation system, a breathing flow simulator, and measurement devices. Such manikin-based system has been used in several earlier studies [7,32–34,65,82]. Figures 2.2a and 2.2b illustrate two set-ups for cyclic flow testing. Within these set-ups, the manikin head was connected to a flow/volume simulator (Series 1120; Hans Rudolph Inc., Shawnee, KS, USA) for the creation of cyclic flows. Figure 2.2a shows the approach in which the exhalation flow was returned to the chamber simulating the actual breathing condition ("inhalation and exhalation" set-up). Figure 2.2b illustrates the approach in which the exhalation flow was exhausted to the outside of the chamber using a three-way pressure valve ("inhalation only" set-up). An extra fan was added in the first set-up (figure 2.2a) to stabilize the concentration variations caused by the exhalation flow returning through the chamber. Figure 2.2c shows the constant flow testing set-up. In this later set-up, an outlet flow pump was used to draw a constant flow through the manikin head. A regulatory pressure valve was used to balance the pressure inside the chamber.

Figure 2.1 – Schematic of the set-up used for evaluating the efficiency of N95 FFRs under constant and cyclic flows [81]

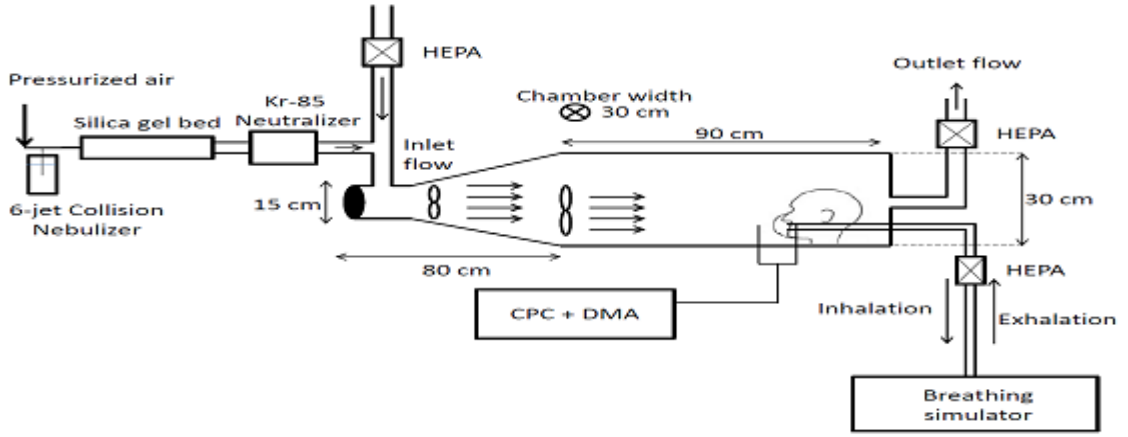

(a)

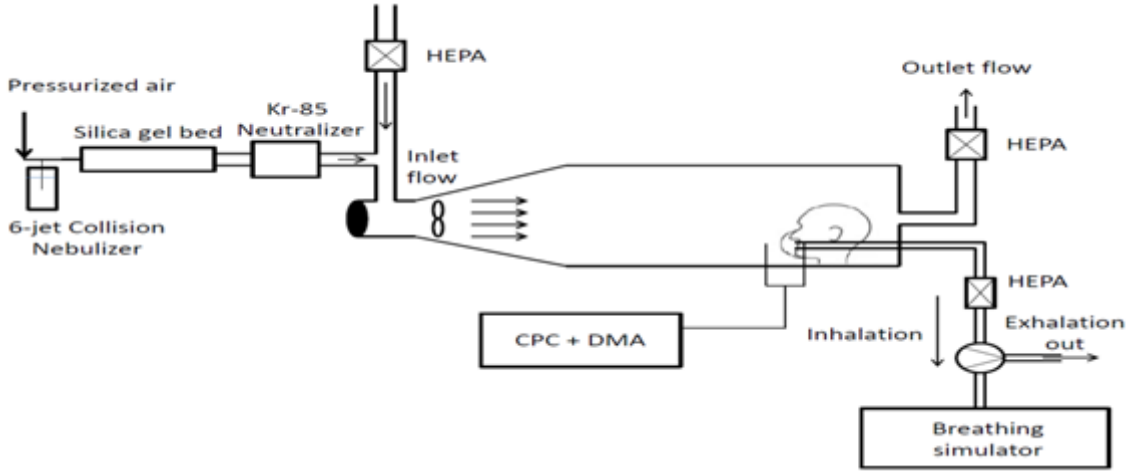

(b)

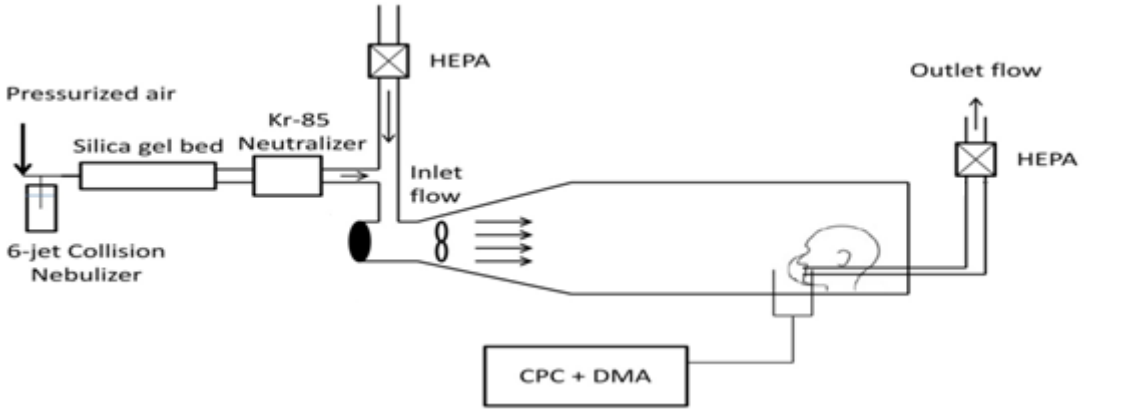

(c)

Figure 2.2 – Experimental set-up for: a) cyclic flow ("inhalation and exhalation" set-up); b) cyclic flow (‘"inhalation only" set-up) and c) constant flow

2.1.2 Particle Generation System

Using a six-jet Collison nebulizer (CN 2425, BGI Inc., Waltham, MA, USA), containing 0.1 % v/v NaCl solution, and a filtered air supply (Model 3074B, TSI Inc., Shoreview, MN, USA), the aerosol flow was provided under 30 psi pressure to generate 10–205.4 nm NaCl polydispersed particles (figure 2.3-a). Afterwards, the flow was passed through the drying system (silica gel packs) to control the humidity of the chamber (figure 2.3-b). Kr-85 electrostatic neutralizer (Model 3012/3012A, TSI Inc., Shoreview, MN, USA) was set to neutralize electrostatic charges carried by the generated particles (figure 2.3c). As discussed in the literature, charged particles could significantly increase the filtration efficiency and not represent the worst-case particle penetration scenario [32,46,47]. The aerosol flow was then diluted by clean air and dispersed through the chamber. An outlet flow with a regulatory valve was used to balance the pressure in the chamber.

a) b) c)

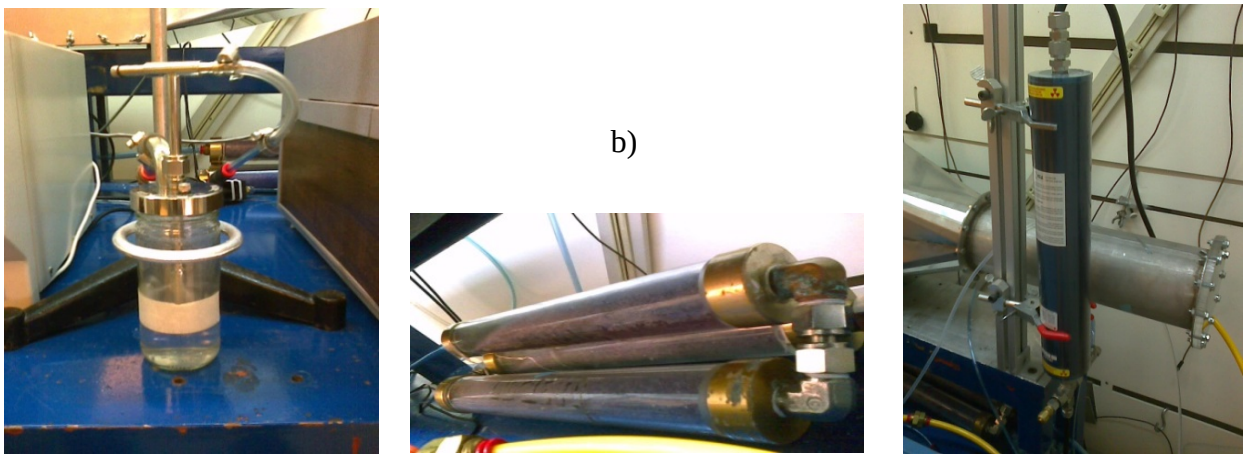

Figure 2.3 – Generation system: a) 6-jet Collison nebulizer, b) drying system (Silica gel bed), and c) Kr-85 electrostatic neutralizer

2.1.3 Measurement Devices

A set of equipment consisting of an “electrostatic classifier” (Model 3080, TSI Inc., Shoreview, MN, USA) containing a long differential mobility analyzer (DMA) and in a condensation particle counter (CPC) (Model 3775, TSI Inc., Shoreview, MN, USA) was used to measure upstream and downstream concentration distribution for either constant or cyclic flow tests (figure 2.4). For a given sample, the DMA classified particles within a certain size range based on their electric mobility diameter. Classified particles were then counted and recorded by the CPC. The technique of concentration measurement through classifying (by DMA) and counting (by CPC) is also referred as scanning mobility particle sizer (SMPS) spectrometry. In each sample, the SMPS data for the tested size range (10–205.4 nm) was divided into 21 size channels. For each experiment, the downstream sample was completed first and then the sample probe was switched towards the upstream direction. The samples were taken during two scans in the downstream direction and two scans in the upstream direction, each scan with a time length of 180 seconds. After each scan, a 15-second retrace time was given by the device for DMA

voltage adjustment, previous air sample clearance and preparation for the new scan. Therefore, the total sampling time (regardless of retrace times) for either downstream or upstream concentration was 360 seconds (two times 180 seconds), which, for cyclic flows, provided at least a 17-second time interval (360 seconds per 21 channel) for recording the concentration of each channel (size).

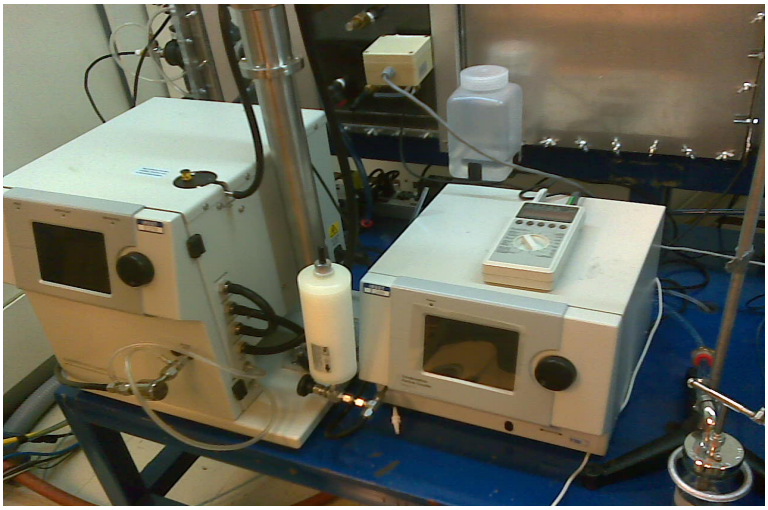

Figure 2.4 – Electrostatic classifier (left) and condensation particle counter (right)

2.2 Penetration Measurement

Particle penetration (P) is defined as the ratio of two concentration distributions:

$$P(\%) = \frac{\left(\frac{dC}{d\log D_p}\right)_d}{\left(\frac{dC}{d\log D_p}\right)_u} * 100\ \% \qquad (1)$$

where C and D_p indicate the number concentration and the particle diameter, respectively; thus the term ($dC/d\log D_p$) represents the number concentration distribution in terms of particle size (#/cm^3). The subscripts *d* and *u* indicate the downstream and upstream filter directions, respectively.

2.3 Measurement Challenges with Cyclic Flow

As previously discussed, penetration is significantly influenced by flow rate, therefore it is expected that the instant penetration is subject to vary during a cyclic flow (where the instant flow rate varies constantly over time). For instance, we can assume that instant penetration reaches a maximum level from zero and then goes back to zero throughout each inhalation cycle (periodically).

The method used to measure the penetration is, as previously mentioned, SMPS spectrometry, since it is an appropriate method for recording polydispersed particles (where concentration is expressed as a function of a size distribution). Nevertheless, SMPS cannot record instant concentrations in terms of particle size. In fact, SMPS records the concentration of each size

channel as an average value over a certain period of time (which is part of a whole SMPS sampling time). To make sure that the given time for SMPS (360 s) provides sufficient time to cover enough flow cycles per channel, penetration measured by the SMPS mode was compared with another mode referred to as "count mode" in the current study. With the count mode, the DMA voltage is set to a constant value to classify only one size of particles (unlike SMPS mode where the DMA voltage is varying in order to record the concentration distribution). The advantage of this mode is that the sampling can be adjusted for any desirable time (however the particle counts are only recorded for one single size). The time intervals can be adjusted down to 0.1 second within the whole sample time in order to estimate the instant counts.

Verifications between the two modes were made for two cyclic flows (with PIFs of 135 and 360 L/min) with the two experimental set-ups ("inhalation and exhalation" set-up, and "inhalation only" set-up). For the count mode, three single sizes of 22.1, 39.2 and 107.5 nm were selected and both downstream and upstream concentrations were measured. For each size and each stream, a period of 2 minutes was given to record an average concentration (a total of 6 minutes for the three sizes). For the SMPS mode, as previously mentioned, a total time period of 360 s was given for each upstream or downstream direction (for the particle size range of 10-205.4 nm). For each flow rate, penetration was measured for one single respirator in both count and SMPS modes. Penetration values were then compared and differences were computed (figures 2.5 to 2.8).

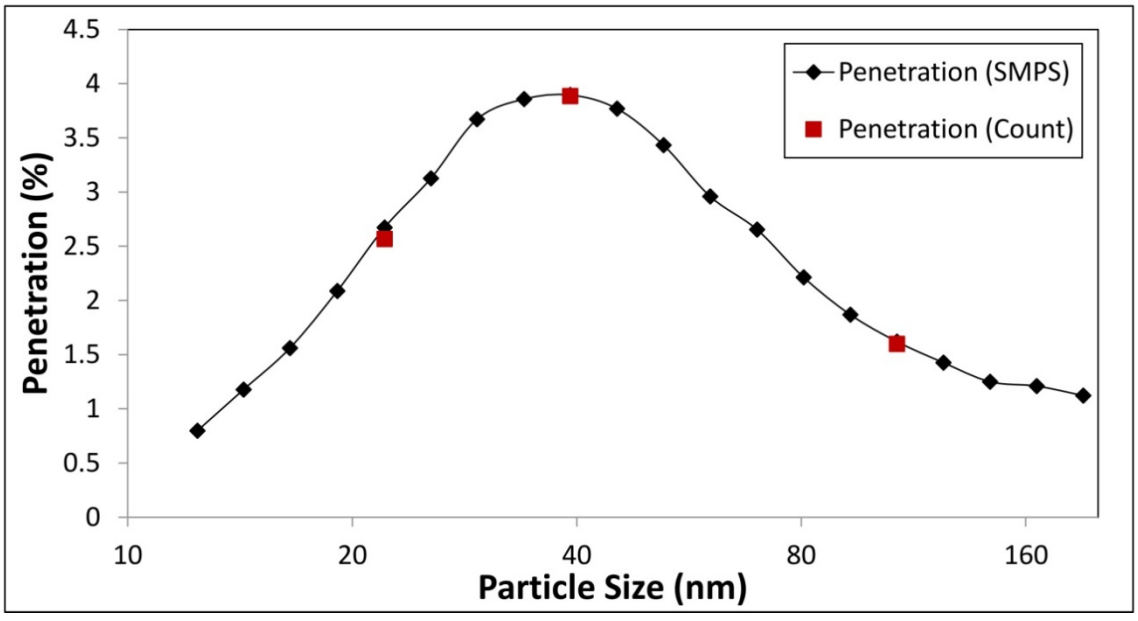

Figure 2.5 – Penetration measured in SMPS and count modes for a cyclic flow rate of 135 L/min as PIF ("inhalation and exhalation" set-up)

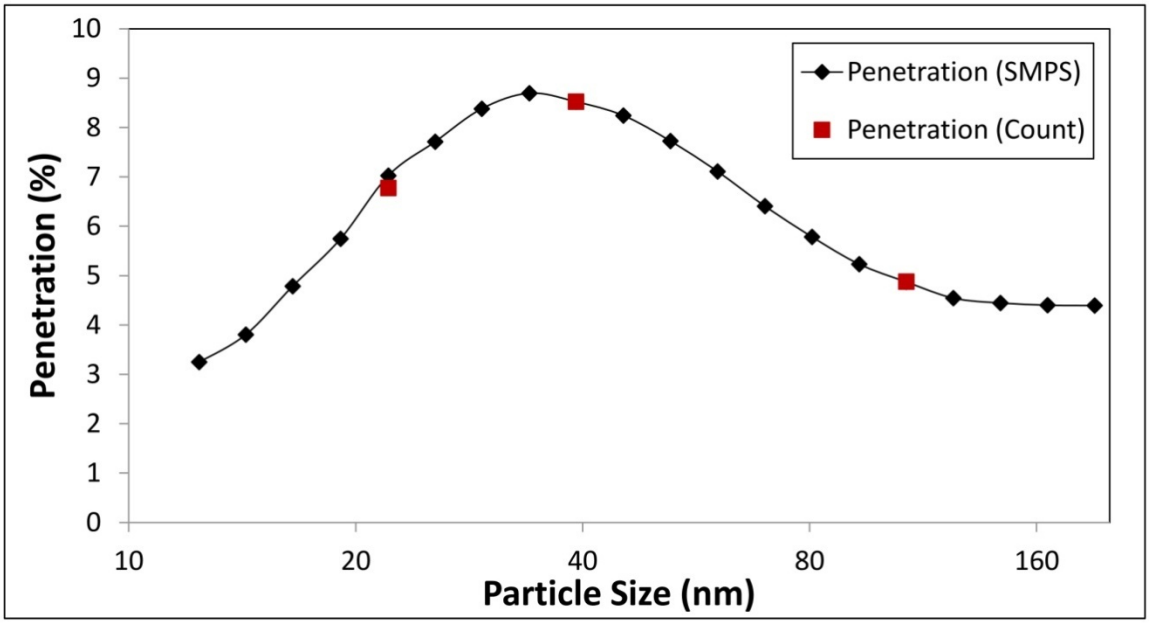

Figure 2.6 – Penetration measured in SMPS and count modes for a cyclic flow rate of 360 L/min as PIF ("inhalation and exhalation" set-up)

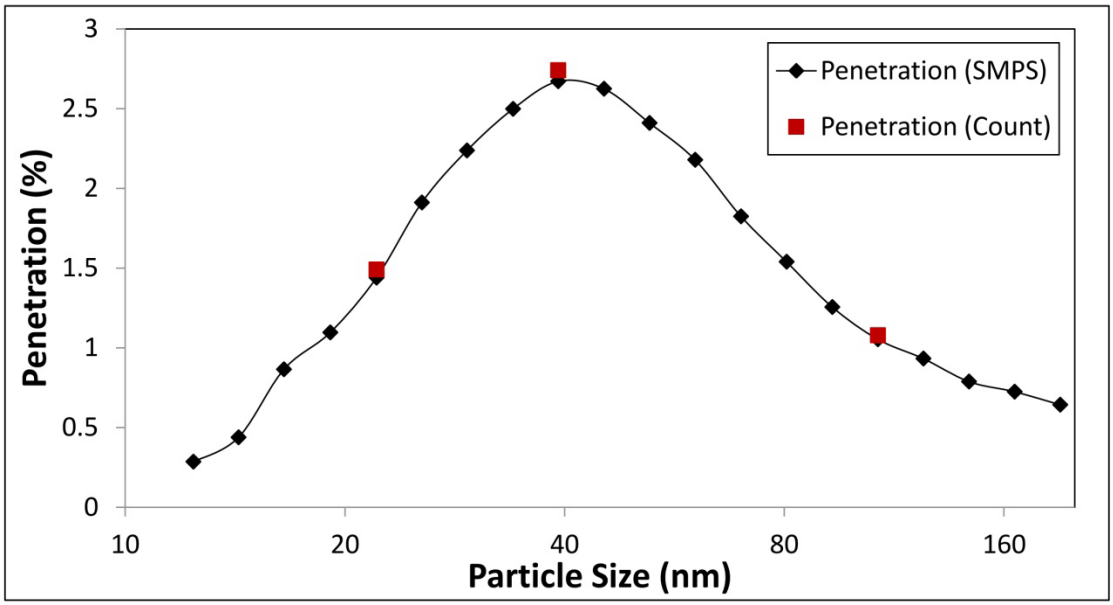

Figure 2.7 – Penetration measured in SMPS and count modes for a cyclic flow rate of 135 L/min as PIF ("inhalation only" set-up)

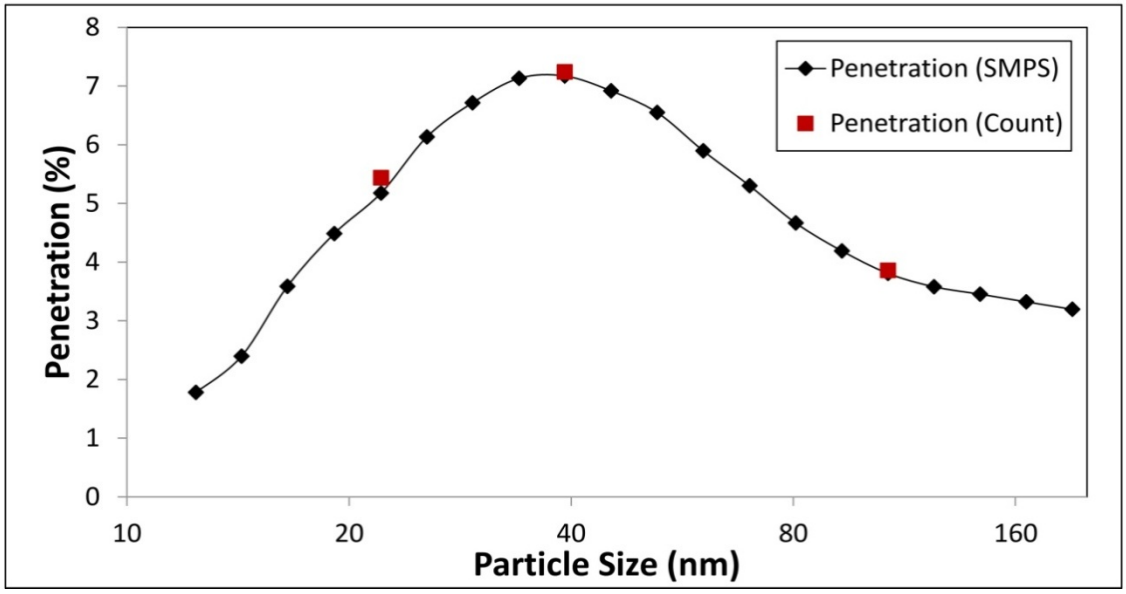

Figure 2.8 – Penetration measured in SMPS and count modes for a cyclic flow rate of 360 L/min as PIF ("inhalation only" set-up)

As seen in figures 2.5 to 2.8, the values for penetration obtained by count and SMPS modes were close to each other. For a cyclic flow rate of 135 L/min with the "inhalation and exhalation" set-up, for instance, the difference errors between penetrations obtained with the two modes was 3.93, 0.26 and 1.3 % for the particles of 22.1, 39.2 and 107.5 nm, respectively. Similarly, for all other flow rates, the difference between penetrations obtained with the two modes was found to be negligible. This validated that, for our flow selections, the sampling time of 360 s for the SMPS mode is appropriate to obtain accurate average values for penetration measurements.

2.4 Set-up Verification Tests

To ensure the accuracy of the penetration measurements, two verification tests were performed for each flow rates selected in this study: a "no-filter" test and a "stability" check.

First, to make sure that there was no significant bias between the downstream and the upstream samples that are measured, upstream and downstream samples were recorded using a manikin head holding no respirator ("no-filter test"). The deviation between two samples throughout all size channels was then evaluated. The aim of the "no filter" test was to check that both upstream and downstream sample probes perform equally by recording the same concentration, thus ensuring that the measured efficiency is completely attributed to the filter (that it is not a fractional efficiency due to differences between the upstream and downstream sample probes). For example, figures 2.9 and 2.10 indicate the "no filter" test results for a constant and a cyclic flow (as minute volume) rates of 85 L/min ("inhalation only" set-up), respectively. Similar "no-filter" tests had also been performed in previous works to check for equality in the upstream and downstream samples [34,60,61].

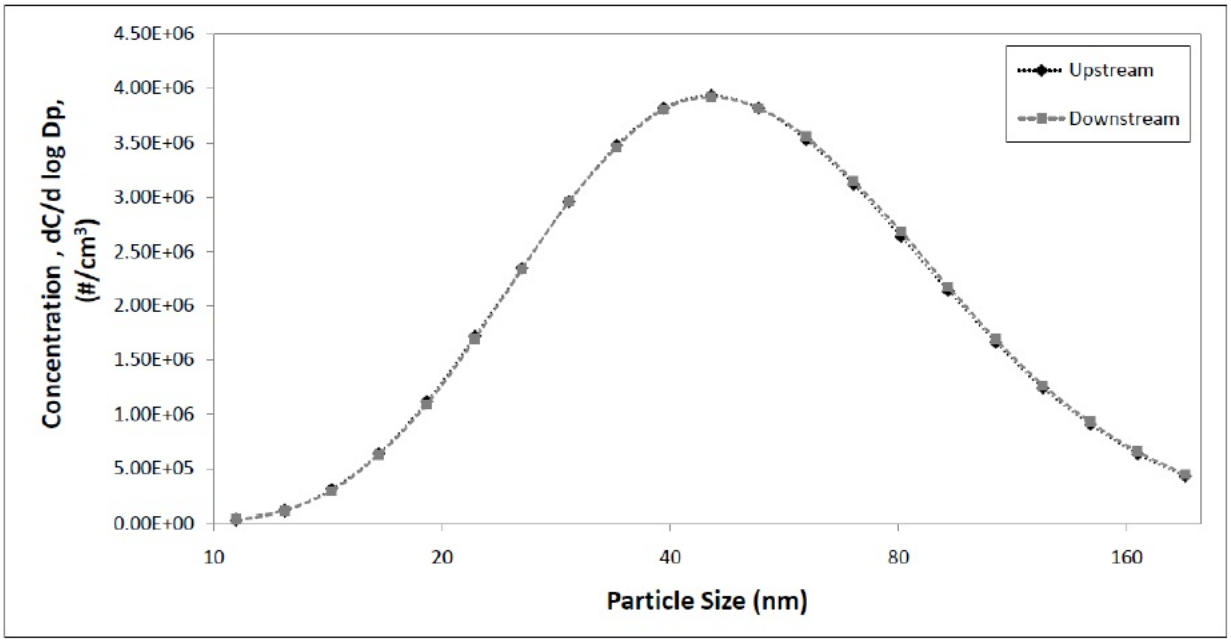

Figure 2.9 – "No filter" test for a constant flow rate of 85 L/min

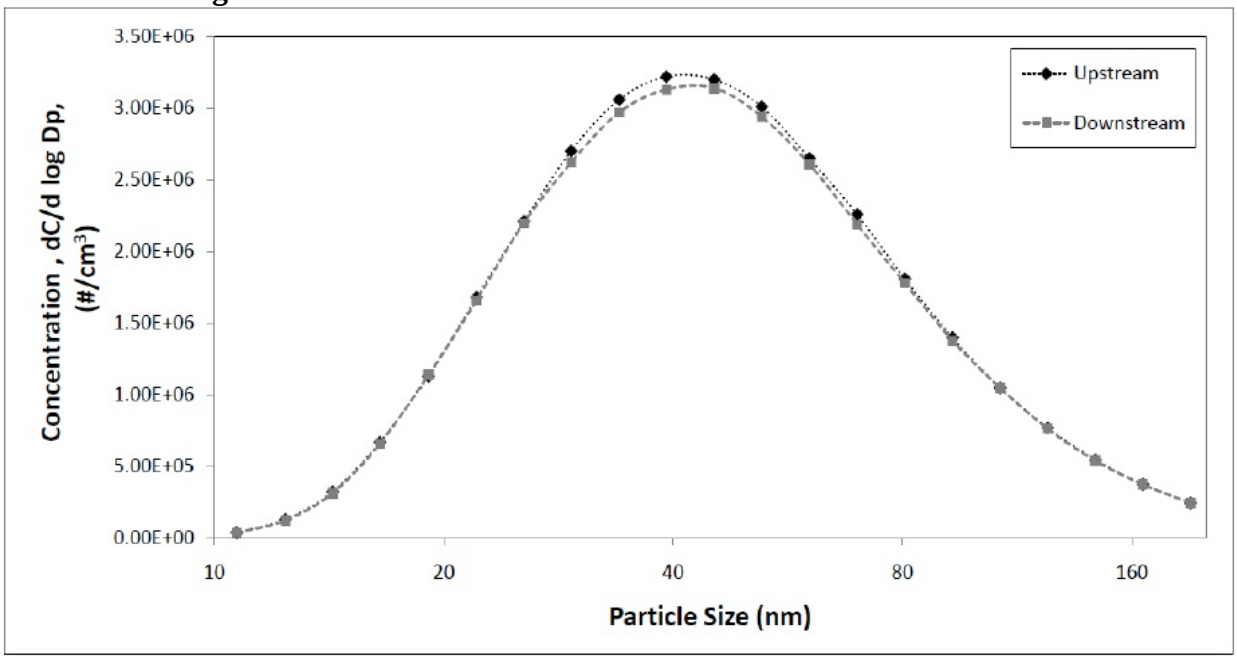

Figure 2.10 – "No filter" test for a cyclic flow rate of 85 L/min (minute volume)

The stability of the upstream concentration inside the chamber was also tested. The aim of this test was to ensure that with the utilized generation system, the concentration remains stable over time, once it reaches equilibrium. Hence, upstream concentrations (after reaching the equilibrium value from zero) at times 0, 15, 30, 45 and 60 minutes were measured for all the selected flow rates. Differences across samples throughout all size channels were assessed. For example,

figures 2.11 and 2.12 illustrate the stability for the constant and cyclic flow (as minute volume) rates of 85 L/min ("inhalation only" set-up).

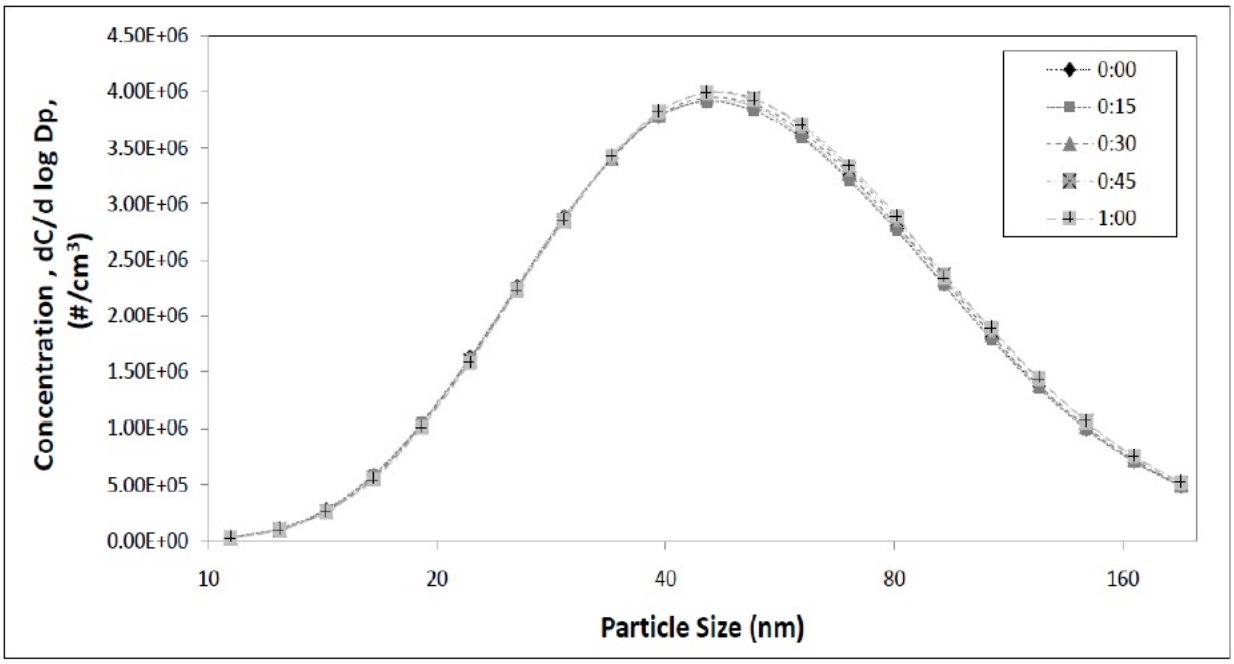

Figure 2.11 – Concentration stability test for a constant flow rate of 85 L/min

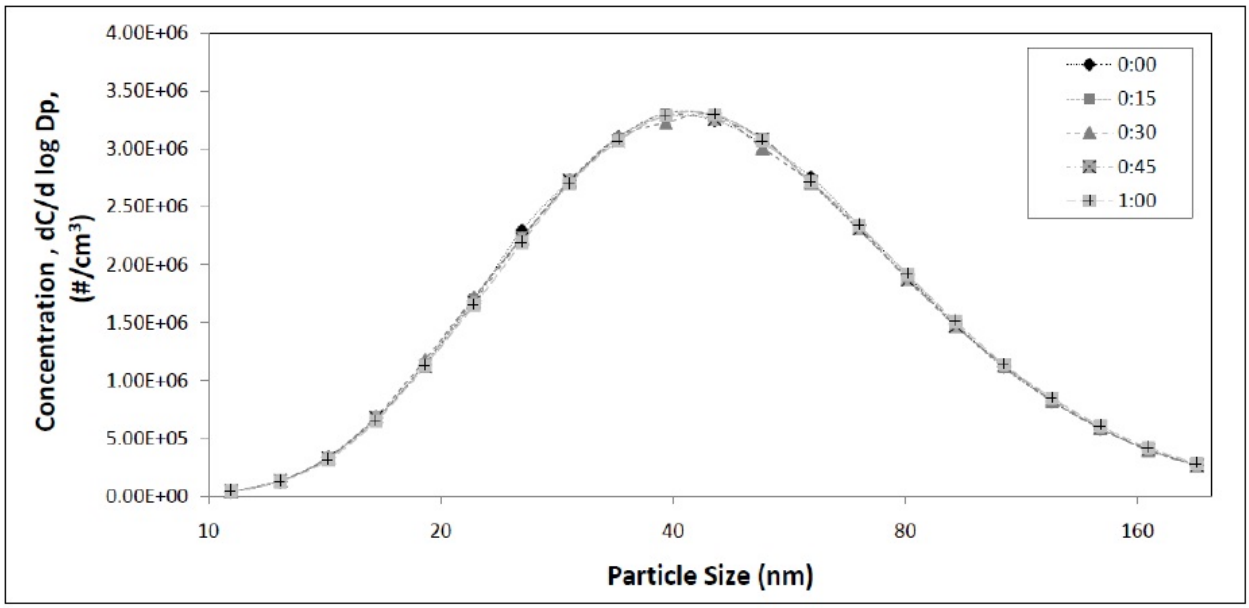

Figure 2.12 – Concentration stability test for a cyclic flow rate of 85 L/min (as minute volume)

With both verification tests, minor deviations were observed among the recorded samples. Indeed, the maximum and average deviations throughout all channels did not exceed 13 and 5 %, respectively. In addition, the deviation at MPPS, which is the most important value in the evaluation of filtration efficiency, was less than 5 %.The maximum deviation in both verification tests normally occurred at the smallest or largest size channels (close to 10 or 205.4 nm, the two extreme sides) where the concentration distribution (in terms of particle size) was very low compared to other size channels. However, the deviations among concentrations in most size channels (including the MPPS) were significantly less than the maximum deviation.

2.5 Respirator Selection

One model of commercially available cup-shaped N95 FFR was considered for the experiments of this study. The respirators were not preconditioned and they were tested as received. After each test, the used respirator was taken off from the manikin and discarded and a new respirator was set for the next test. Each respirator was suitably sealed to the manikin by a silicone sealant to avoid any potential leakage. Therefore this study does not address the leakage pathways for penetration of UFPs.

2.6 Experimental Protocols

2.6.1 Contribution of Frequency and PIF

2.6.1.1 Enhancement Fraction Values

For a given size and filter, the magnitude of penetration under a sinusoidal cyclic flow is a function of breathing frequency (Fr) and PIF, assuming all other parameters, such as humidity, temperature, loading time and loaded mass are constant. One can write:

$$P = f(PIF, Fr) \quad (2)$$

In such a scenario, the variations in penetration due to PIF and Fr can mathematically be expressed as:

$$dP = \left(\frac{\partial P}{\partial PIF}\right)_{Fr} d(PIF) + \left(\frac{\partial P}{\partial Fr}\right)_{PIF} d(Fr) \quad (3)$$

And the total penetration variation can be obtained by:

$$\int dP = \int \left(\frac{\partial P}{\partial PIF}\right)_{Fr} d(PIF) + \int \left(\frac{\partial P}{\partial Fr}\right)_{PIF} d(Fr) \quad (4)$$

or

$$\Delta P_{tot} = \Delta P_{PIF} + \Delta P_{Fr} \quad (5)$$

The term ΔP_{tot} is the total penetration variation, and ΔP_{PIF} and ΔP_{Fr} are the individual penetration variations caused by changes in the PIF and Fr, respectively. Figure 2.13 illustrates Eq. 5 graphically. It shows that the total penetration variations can be estimated by adding the impact

of individual PIF and frequency. This is obtained from the difference in penetrations measured between points D and A (where both Fr and PIF have changed, as it occurs in a real respiration path). The individual effect of PIF can be estimated by the difference in penetrations between points A and C, or B and D. Similarly, the individual effect of Fr can be measured by the difference in penetrations between points A and B or C and D.

The ratio of individual penetration variation for each contributor to the total penetration variation is defined as the enhancement fraction value:

$$X_{PIF}(\%) = \frac{\Delta P_{PIF}}{\Delta P_{tot}} * 100\ \% \quad (6)$$

$$X_{Fr}(\%) = \frac{\Delta P_{Fr}}{\Delta P_{tot}} * 100\ \% \quad (7)$$

where X_{PIF} and X_{Fr} represent the portions of penetration enhancement due to PIF and breathing frequency, respectively.

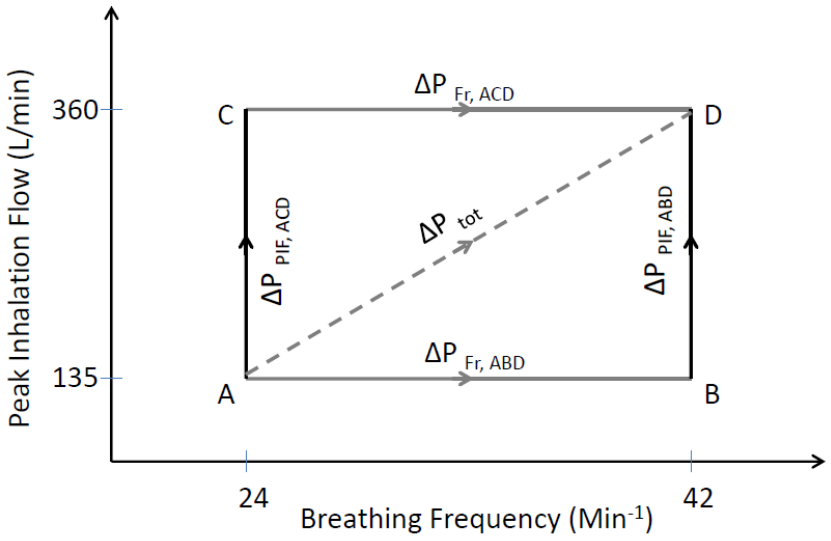

Figure 2.13 – Penetration variation in terms of frequency or PIF

2.6.1.2 Experimental Conditions

Figure 2.14 shows four different cyclic flows (with sinusoidal pattern) used for this part of the study, consisting of two breathing frequencies (24 and 42 BPM) and two PIFs (135 L/min and 360 L/min). The summary of information regarding the cyclic flows selected is given in table 2.1 (flows A, B, C and D). The tests were performed with both cyclic flow set-ups: “inhalation and exhalation” and “inhalation only” (see figure 2.2 a,b).

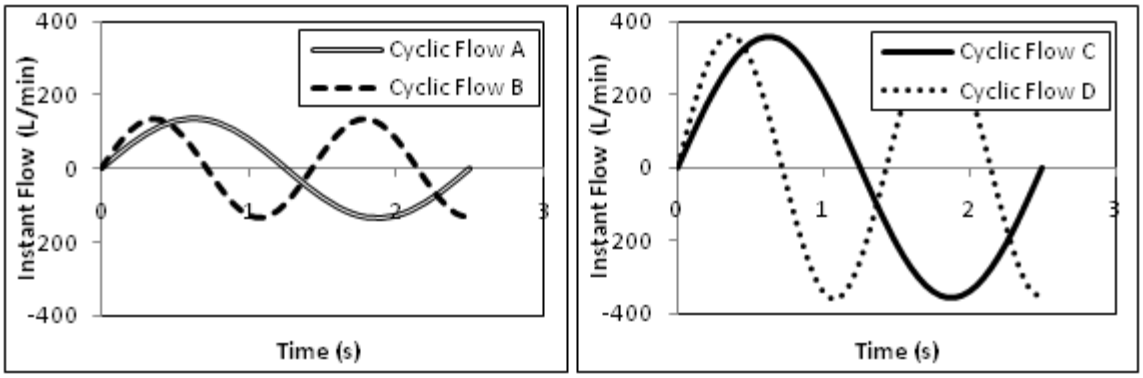

Figure 2.14 – Cyclic flow patterns used

Table 2.1 – Cyclic flow selections

Cyclic Flow	Breathing Frequency (BPM)	Peak Inhalation Flow, PIF (L/min)	Tidal Volume (L)
A	24	135	1.771
B	42	135	1.013
C	24	360	4.792
D	42	360	2.741

The values of 135 and 360 L/min as PIF were selected to make an appropriate relevance to the real-world situation during respiration with moderate to heavy workloads, respectively. For instance, 135 L/min as PIF (equal to 42 L/min as minute volume) is a good approximation for moderate ventilation as Caretti *et al.* and Anderson *et al.* suggest values of 38.5 and 47.4 L/min (minute volume), respectively [74,76]. These suggestions were based on physiological data obtained from human subjects exercising under various workloads. Based on the appropriate relevance of cyclic flow with 135 L/min as PIF to the workplace breathing conditions, it has frequently been selected by several investigators for filter efficiency evaluations [60–62,67,74]. The breathing frequency of 24 BPM selected for the current study is also within the reported range of breathing rate suggested by Anderson *et al.* (26.5 ± 6.7 BPM) [73]. Although the occurrence of 360 L/min is not as frequent as 135 L/min, it has been reported by physiological literature during heavy workload respiration. The value of 360 L/min (equal to 114 L/min as minute volume) corresponds to the average of the maximum flow rate measured at the end of the exercise with a maximum workload performed on different human subjects [73]. The corresponding breathing frequency of 42 BPM was observed with this breathing flow. Almost a similar number (363.9 L/min as PIF) was suggested by Berndtsson utilizing full-face masks for healthy human subjects when breathing in case of heavy workload [83]. As for the 135 L/min, the value of 360 L/min has also been used for filter efficiency evaluation in other relevant studies [34,64]. Overall, the selected PIFs and breathing frequencies used in this study cover breathing from a moderate to heavy workloads. The negative values of instant flow (exhalation cycle) in figure 2.14 are assumed to be zero for the “inhalation only” set-ups, since exhalation was

eliminated from the cyclic flow. Temperature and RH in the chamber, in this part of the study, were 25 ± 3 °C and 15 ± 5 %, respectively.

2.6.1.3 Data Analysis

Each penetration measurement (polydispersed; 10-205.4 nm) was repeated with four different batches of respirators, and represented by the mean value and the standard deviation. Each experiment was repeated for the "inhalation and exhalation" and the "inhalation only" set-ups (see figure 2.2a,b) for which the experimental parameters were randomly varied (N=4 for each experimental condition). The selection of flows A and D (see table 2.1) reflects the fact that, in practice, breathing frequency and PIF simultaneously increase. In order to consider the individual effects of frequency and inhalation flow, only one parameter was varied, while the other was kept constant. Flows B and C were then added. Consequently, according to figure 2.9, the two following paths could separately address the impact of frequency and PIF:

1. Path ABD: First, increasing breathing frequencies only (from 24 to 42 BPM, while PIF is kept at 135 L/min), and then increasing PIF only (from 135 to 360 L/min while breathing frequency is kept at 42 BPM). The corresponding penetration differences are referred as $\Delta P_{Fr,ABD}$ and $\Delta P_{PIF,ABD}$, respectively.

2. Path ACD: First, increasing PIF only (from 135 to 360 L/min while breathing frequency is kept at 24 BPM), and then increasing breathing frequency (from 24 to 42 BPM while PIF is kept at 360 L/min). Corresponding penetration differences are cited as $\Delta P_{PIF, ACD}$ and $\Delta P_{Fr, ACD}$, respectively.

In addition to penetration values, the MPPS range was obtained for each cyclic flow. Enhancement fraction values (X_{PIF} and X_{Fr}) were then calculated (by dividing ΔP_{PIF} and ΔP_{Fr} by the total penetration variation (ΔP_{tot})) for the MPPS range, based on the two paths introduced above.

Using NCSS Program Software (NCSS, LLC Inc., Kaysville, UT, USA), multiple comparison tests were applied through analyses of variance (ANOVA) to check the significance of potentially affecting parameters such as breathing frequency, PIF, experimental set-up, and their interactions on the level of particle penetration in the MPPS range. The values obtained for penetration in the MPPS range were transformed to their logarithmic values as the dependent variable in the ANOVA. For each experimental set-up, a separate two-way ANOVA for PIF and breathing frequency was performed. Finally, a three-way ANOVA combining the data between "inhalation and exhalation" and "inhalation only" set-ups were applied to examine the impact of the experimental set-up. Using descriptive statistics for each analysis, the normality of transformed penetrations was accepted by the Martinez-Iglewicz normality test.

2.6.2 Comparison of Constant and Cyclic Flows

2.6.2.1 Experimental Conditions

Four cyclic flows with PIFs of 135, 210, 270 and 360 L/min (indicated by groups G3 to G6 in table 2.2) were primarily chosen. The corresponding breathing frequencies for these flows were

24, 30, 36 and 42 BPM. For this objective, the tests for cyclic flows were performed with the "inhalation only" set-up.

Table 2.2 – Constant and cyclic flow selections

Flow group	Cyclic flow [Fr[a] (BPM), PIF[b] (L/min)]	Constant flow		
		Equal to cyclic flow minute volume (L/min)	Equal to cyclic flow MIF[c] (L/min)	Equal to cyclic flow PIF (L/min)
G1	Fr=16, PIF=68	N/A	42	68
G2	Fr=20, PIF=105	N/A	68	N/A
G3	Fr=24, PIF=135	42	85	135
G4	Fr=30, PIF=210	68	135	210
G5	Fr=36, PIF=270	85	170	270
G6	Fr=42, PIF=360	115	230	360
G7	Fr=45, PIF=430	135	270	N/A
G8	Fr=48, PIF=570	N/A	360	N/A

a) Fr: Breathing frequency (breaths per minute)
b) PIF: Peak inhalation flow
c) MIF: Mean inhalation flow

The rationale for the selection of the cyclic flows was previously explained (section 2.6.1.2) for the 135 and 360 L/min flow rate. The cyclic flow of 270 L/min as PIF was selected to introduce a cyclic flow corresponding to 85 L/min as minute volume (as certified by NIOSH). The cyclic flow of 210 L/min as PIF was selected as it simulates the mean breathing flow measured under heavy workload, as reported by Anderson *et al.* (mean PIF of 218.4 ± 53.7 L/min with a corresponding breathing frequency of 31.9 ± 7.4 BPM) [73].

Penetration values obtained for each of the above-mentioned cyclic flows were accompanied by the measurement of penetration achieved under three constant flows equivalent to minute volume, MIF and PIF of the same cyclic flow (flows indicated in the same row in table 2.2). To have a large set of data for comparing cyclic flows and constant flows equal to cyclic flow MIF, another four cyclic flows possessing equivalent MIFs of 42, 68, 270 and 360 L/min were selected (table 2.2). They were presented in groups G1, G2, G7 and G8, respectively. The corresponding PIF for these flows were 68, 105, 430 and 570 L/min. The first two flows reflect normal breathing achieved by sedentary to moderate workload breathing. The cyclic flow with 430 L/min as the PIF corresponds to the upper standard deviation of breathing during the highest workload (363.9 ± 66.3 L/min), as reported by Berndtsson [83]. A similar value has also been reported by Blackie *et al.* [73]. The cyclic flow of 570 L/min may also represent the upper 95 % percentile of high workload breathing when subjects speak during exercise (reported as 573

L/min by Berndtsson [83]). The RH and the temperature of the chamber were kept at 15 ± 5 % and 25 ± 3 ºC, respectively.

2.6.2.2 Data Analysis

Penetration measurements were carried out for both cyclic and constant flows. For each flow rate, five different batches of respirators (N=5) were randomly tested and the corresponding initial penetration values were represented by their means value and standard deviation. Subsequently, for each flow, the MPPS was obtained. For comparison of the penetration achieved by the cyclic flow and by the constant flow equivalent to cyclic MIF, the statistical analysis was performed by one-way and two-way ANOVA. First, comparisons for maximum penetration (response variable) were executed by one-way ANOVAs with the pattern of flow rate (cyclic or constant) as the factor variable. Second, a two-way ANOVA was carried out to investigate the impact of factor variables: flow rate magnitude, flow rate pattern (cyclic or constant) and their interaction on the maximum penetration (response). For the two-way ANOVA the data corresponding to constant and cyclic flow rates (with the same MIF) of 42 and 68 L/min were not considered by the analysis in order to keep the data within a normal distribution, since a significant deviation from the normal distribution took place when the penetration data for these flow rates was included in the analysis.

2.6.3 Loading Time

2.6.3.1 Experimental Conditions

Two constant flows with magnitudes of 85 and 170 L/min and a cyclic flow with PIF of 270 L/min (minute volume of 85 L/min) were selected. All tests for cyclic flows were performed with “inhalation only” set-up. Penetration was obtained at the initial time (zero) as well as at specific times of 2, 4 and 6 hours from the initial time of the test. The loading tests were performed for three different RH levels: 10, 50 and 80 %. The upstream concentration distribution was polydispersed (GSD ≈ 1.7). The CMD at 80 % RH was, however, observed to be larger (≈ 65-70 nm) compared to the CMD at 10 and 50 % RH (≈ 45 nm).

To make sure that the upstream concentration was in an appropriate stable condition during the 6-hour test, the four recorded upstream concentration distributions (measured at initial time, 2, 4 and 6 hours) were compared with each other and the deviation among the four samples were evaluated. These verifications indicated a relatively stable condition. For instance, for 10 and 50 % RH, the maximum and the average deviations among the samples did not exceed 17 and 8 %, respectively, suggesting that the upstream concentration has been relatively stable during the whole test time.

The maximum deviation normally occurred in the smallest or largest size channels (close to 10 or 205.4 nm) where the concentration distribution (in terms of particle size) was low compared to the other size channels. Nevertheless, the deviations among samples throughout most of the inner channels (including the MPPS, as the worst-case scenario penetration measurement) were significantly less than the maximum deviation. Similar to 10 and 50 % RH, the concentration at 80 % RH was almost stable for all the channels larger than 15 nm.

2.6.3.2 Data Analysis

For each selected flow rate, five different batches of respirators were tested, each for a loading time period of 6 hours. Each of the 6-hour tests was done for three RH levels (10, 50 and 80 %). The experimental parameters were randomly varied throughout the protocol (N=5 for each experimental condition). Penetration values for each flow rate and each loading time were represented by the mean value and its standard deviation. The comparison tests were performed with one-way and two-way ANOVAs to verify the significance of the factors and their interactions on maximal penetration at MPPS. The effect of loading time (at initial, 2, 4 and 6 hours) was verified by a one-way ANOVA for each selected flow and each RH level. The simultaneous impact of flow rate pattern (constant or cyclic) and loading time was also considered using a two-way ANOVA (where the constant flow in this latter analysis was equivalent to the MIF of the cyclic flow). Logarithmic transformations were performed to normalize the pooled data in cases where the normality of the pooled data was rejected by the descriptive statistics.

3 RESULTS AND DISCUSSION

3.1 Contribution of Breathing Frequency and PIF on the Efficiency of N95 FFRs

The data reported in this section has been published in the Annals of Occupational Hygiene (Mahdavi *et al.* [81]).

3.1.1 Results for the "Inhalation and Exhalation" Set-up

3.1.1.1 Penetration vs. PIF and Breathing Frequency

Figure 3.1 illustrates the challenge concentration distributions in terms of particle size at the N95 FFR upstream for the four cyclic flows A, B, C and D. The summary of statistical information for each concentration curve is given in table 3.1.

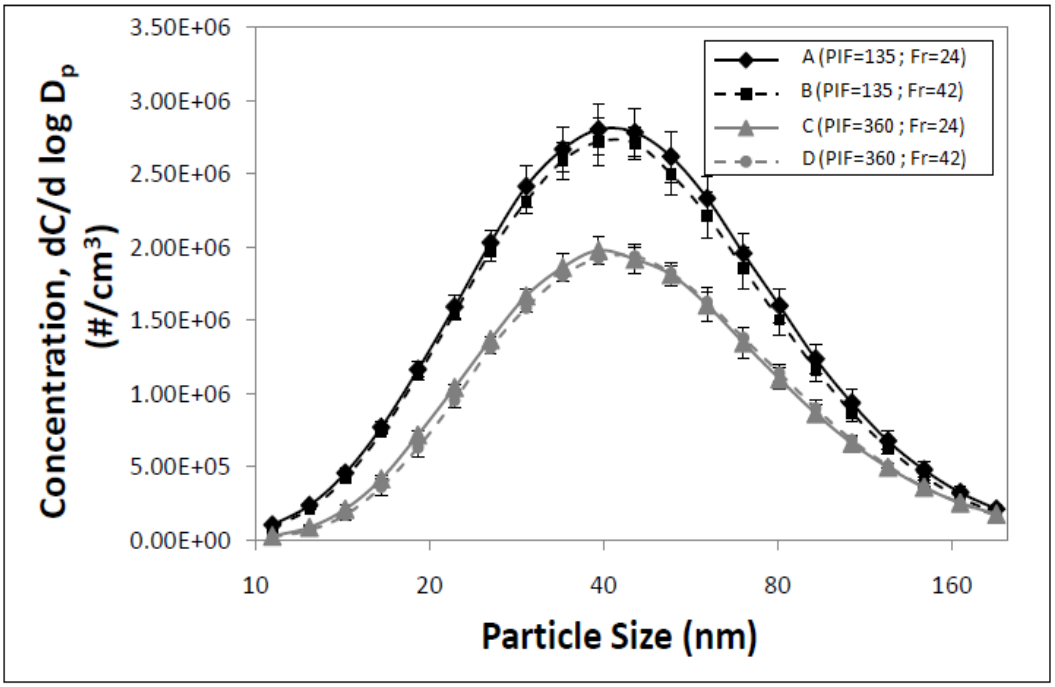

Figure 3.1 –Typical concentration distribution at N95 FFR upstream for the four tested flows for the "inhalation and exhalation" set-up

Table 3.1 – NaCl challenge concentration distribution characteristics for the "inhalation and exhalation" set-up

Cyclic Flow	Count Median Diameter (nm)	Geometric Standard Deviation	Peak concentration ($x10^6$ #/cm^3) (@ peak size in nm) dC/d logDp	Total concentration* ($x\ 10^6$ #/cm^3)
A (PIF=135, Fr=24)	43.3	1.79	2.80 (@ 39.2)	1.84
B (PIF=135, Fr=42)	43.1	1.77	2.72 (@ 39.2)	1.76
C (PIF=360, Fr=24)	44.3	1.77	1.98 (@ 39.2)	1.25
D (PIF=360, Fr=42)	45.6	1.75	1.94 (@ 45.3)	1.23

* Normalized by log D_p

Figure 3.2 reports the penetration of 10–205.4 nm NaCl particles through the tested N95 FFRs for all the tested cyclic flows. The maximum values for the penetrations normally occurred within the range of 29.4–39.3 nm (MPPS range). As illustrated, compared with the flow A (lowest frequency and PIF), penetrations under flows B, C and D showed an increase. This suggested that both frequency and PIF could be influential in enhancing the magnitude of penetration; nonetheless, the impact of PIF was observed to be much more pronounced than the impact of frequency. For path ABD (see figure 2.10) for instance, the average penetration at MPPS reached 3.31, 3.66 and 9.22 % for the three cyclic inhalation flows A, B and D, respectively. This corresponds to only an 11 % increase in penetration when the frequency was changed from 24 to 42 BPM (point A to point B) while keeping the same PIF. But a 152 % increase in penetration occurred when the PIF was increased from 135 to 360 L/min (point B to point D) while keeping the frequency constant. Similarly for path ACD (where penetration of the MPPS range under flow C reached 7.92 %), a 139 % increase in penetration was observed when the PIF was changed from 135 to 360 L/min (point A to point C), and only 16 % when the frequency was varied from 24 to 42 BPM (point C to point D). These percentages suggest that the impact of breathing frequency on penetration increase is almost negligible compared with the PIF. Statistical analysis, achieved by two-way ANOVA, confirmed the significant impact on penetration as a result of PIF ($p<0.001$), and the insignificant impact due to Fr ($p=0.123$). The analysis suggested no significant interaction between these two parameters ($p=0.764$).

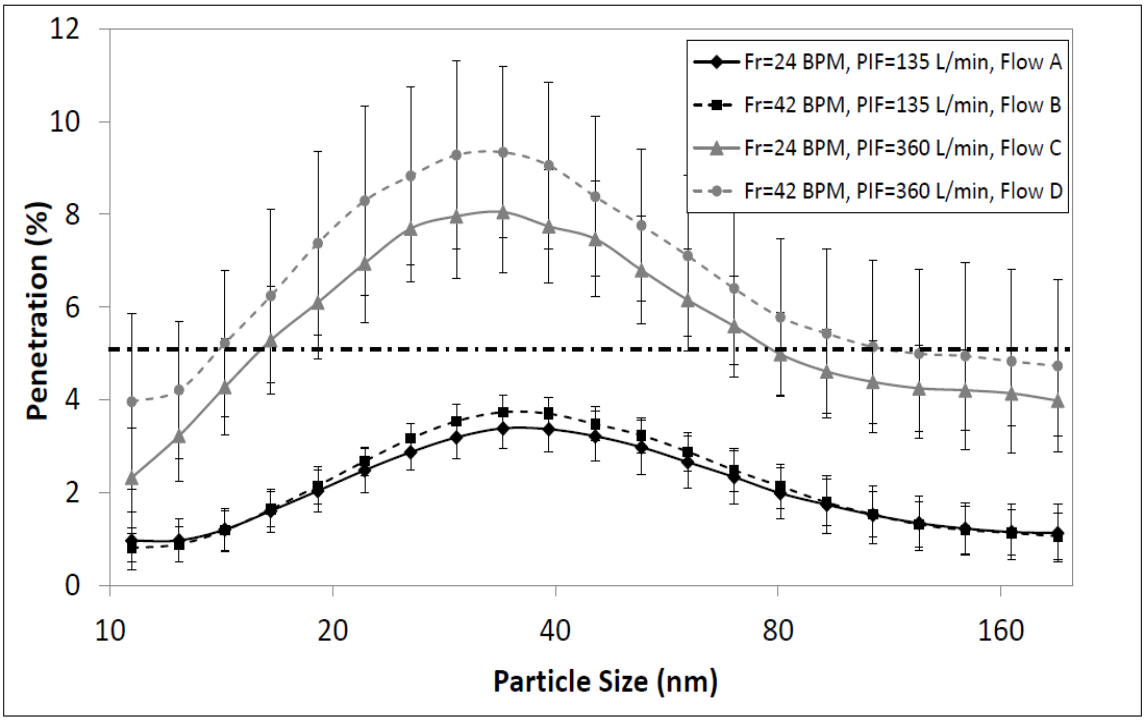

Figure 3.2 – Particle penetration for the four tested cyclic flows for the "inhalation and exhalation" set-up. The dashed line indicates the NIOSH 5 % limit for N95 FFRs (42 CFR, 84)

3.1.1.2 Enhancement Fraction Values

The enhancement fraction values (X_{PIF} and X_{Fr}) can help in interpreting the relative contribution of PIF and breathing frequency as the characteristic properties of breathing flow. For path ABD (see figure 2.10), the frequency enhancement fraction value did not exceed 6 % and the rest of the enhancement (94 %) was due to PIF variations. The same qualitative results (higher PIF fractions) were also recorded for path ACD where 22 and 78 % were respectively calculated as frequency and PIF enhancement fractions. This is showing that the impact of PIF is more pronounced compared with breathing frequency. In a real respiratory trend, inhalation flow rate and breathing frequency increase simultaneously. Hence any change in penetration could be attributed to both parameters. The enhancement fraction values help interpreting the results suggesting that the penetration increase is mostly due to one of the two parameters (namely PIF), and that the impact of the other parameter (breathing frequency) can be neglected.

3.1.2 Results for the "inhalation only" set-up

3.1.2.1 Penetration vs. PIF and Breathing Frequency

The same approach used for the "inhalation and exhalation" scenario was applied to the case of "inhalation-only" set-up. The challenge concentration distributions and the statistical information are available in figure 3.3 and table 3.2

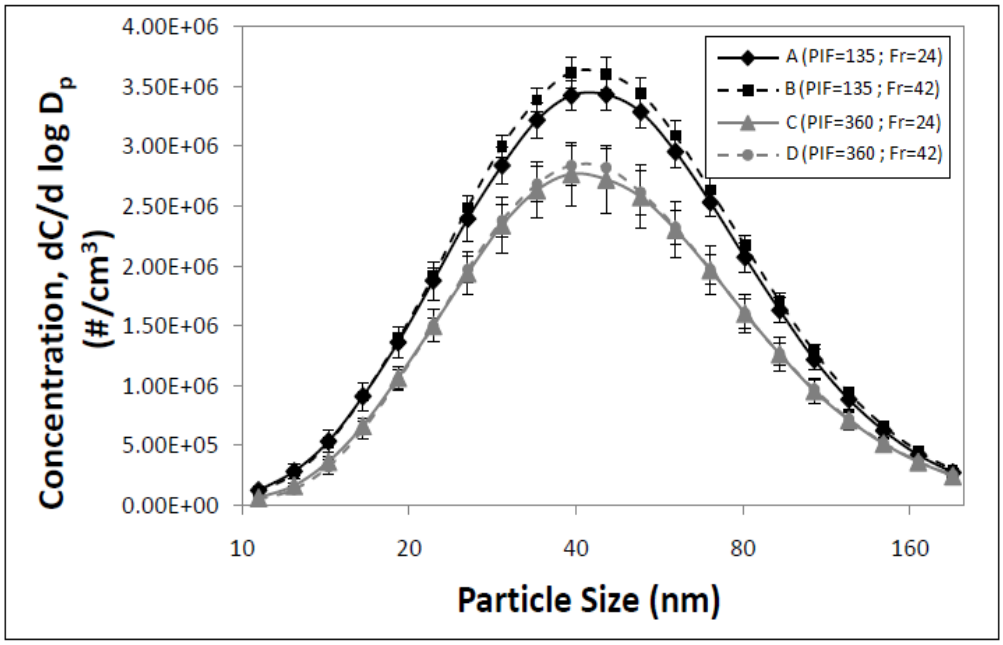

Figure 3.3 – Typical concentration distribution at N95 FFR upstream for the four tested flows for the "inhalation only" set-up

Table 3.2 – NaCl challenge concentration distribution characteristics for the "inhalation only" set-up

Cyclic Flow	Count Median Diameter (nm)	Geometric Standard Deviation	Peak concentration ($x10^6$ #/cm^3) (@ peak size in nm) dC/d log D_p	Total concentration* ($x\ 10^6$ #/cm^3)
A (PIF=135, Fr=24)	44.5	1.79	3.43 (@ 45.3)	2.27
B (PIF=135, Fr=42)	44.7	1.78	3.62 (@ 39.2)	2.37
C (PIF=360, Fr=24)	44.4	1.78	2.77 (@ 39.2)	1.80
D (PIF=360, Fr=42)	44.5	1.77	2.84 (@ 39.2)	1.81

* Normalized by log D_p

Figure 3.4 illustrates the penetrations measured within the entire tested range (10–205.4 nm) for the four selected cyclic flows for the "inhalation only" set-up. Penetration normally reached its highest values within the range of 29.4–39.3 nm (MPPS). Indeed, the maximal penetrations were 2.99, 3.28, 7.31 and 8.02 % for the four tested conditions respectively. This suggests a 10 % increase in the penetration when the frequency is increased from 24 to 42 BPM (path ABD in figure 2.10, from flow A to flow B). On the other hand, a 145 % increase was observed by increasing the PIF from 135 to 360 L/min (from flow B to flow D). Similarly, a 144 % increase in penetration was observed when the PIF was increased from 135 to 360 L/min (path ACD, from flow A to flow C). It is also shown that only a 10 % increase was observed when the frequency was varied from 24 to 42 BPM (from flow C to flow D). Using a two-way ANOVA, a

statistically significant change in penetration is measured through PIF variations ($p<0.001$) while the change caused by frequency is not significant ($p=0.332$). As it was the case when using "inhalation and exhalation", no effective interaction was detected between the two parameters ($p=0.987$) when using the "inhalation only" set-up.

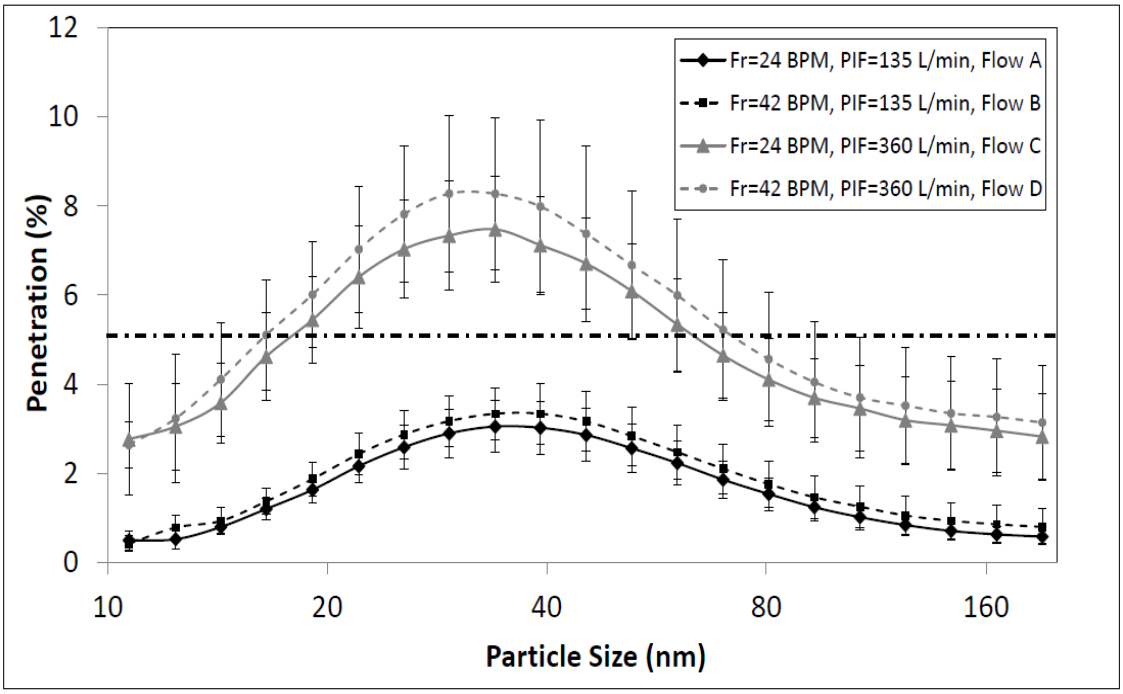

Figure 3.4 – Particle penetration in terms of particle size, for the four tested cyclic flows for the "inhalation only" set-up. The dashed line indicates the NIOSH 5 % limit for N95 FFRs (42 CFR, 84)

3.1.2.2 Enhancement Fraction Values

Similar methodology, used in the "inhalation and exhalation" set-up for the calculation of enhancement fraction values (X_{PIF} and X_{Fr}), was applied with the "inhalation only" set-up to investigate the contribution of frequency and PIF. For instance, for path ABD (see figure 2.10), the frequency and PIF enhancement fractions were 6 and 94 %, respectively. Similarly, 14 and 86 % were respectively calculated as frequency and PIF enhancement fractions for path ACD.

The dashed line in figures 3.2 and 3.4 shows the NIOSH 5 % limit for N95 FFRs (42 CFR, 84). It should however be noted that the current test protocol is different from the NIOSH certification. First, NIOSH uses a constant flow with a rate of 85 L/min rather than a cyclic flow. Second, NIOSH measures the penetration at an MMD of 300 nm, based on the light scattering method to record the concentration upstream and downstream for particle sizes which should represent the worst-case scenario. In this study, polydispersed particles were analyzed using the SMPS. As seen in figure 3.2 for "inhalation and exhalation" set-up, penetration of particles were reported above 5 % within the 16.5–80.6 nm range for case C (PIF=360, Fr=24), and 14.3–107.5 nm for case D (PIF=360, Fr=42). This shows that under high PIFs (360 L/min), the range of UFPs penetration exceeds the NIOSH threshold limit when the MPPS is considered. The raise of penetration by increasing the PIF is attributed to the fact that with higher inhalation flows, the

rate of the major capturing mechanisms (electrostatic and diffusion) is considerably reduced. This is consistent with the results of previously published works for cyclic flows at higher PIF values [60,61,64,66]. On the other hand, penetration does not exceed the 5 % limit at 135 L/min PIF for all frequencies. The observed low variation in penetration, as a function of different frequencies (in the nanometer range), is consistent with the results of Wang *et al.* [66] (tested for 0.3 µm size) and He *et al.* [70]. As reported in previous papers [31-34,43,64] and confirmed in our study, the MPPS was below 100 nm for all selected flows, which confirms the presence of electrostatic charges in the tested N95 FFRs.

3.1.3 Impact of Experimental Set-up

As stated earlier, two different experimental set-ups were used in this study: the first set-up included both inhalation and exhalation through the filter media, while the second set-up included only inhalation. Even though we observed almost similar results from the two experimental set-ups, we did notice a systematic difference in the penetration: the penetration values for the first setup ("inhalation and exhalation") were slightly higher than the values for the second setup ("inhalation only"). However, it should be noted that the statistical analysis indicated that such an increase is not significant. The results of one-way ANOVA test with the experimental setup as the factor variable indicated the impact of experimental set-up is not significant for each selected flow rate ($0.306 \leq p \leq 0.535$). The three-way ANOVA test also indicated a substantial impact by PIF ($p<0.001$); but compared to PIF, the impact of frequency ($p=0.078$) and experimental setup ($p=0.071$) was not significant. Also, no effective interaction was detected between any of these factors ($0.778 \leq p \leq 0.968$). Among the different possible explanations of this situation, the slight increase in penetration for the first set-up ("inhalation and exhalation") could potentially be attributed to the fact that the exhaled air may remove some of the particles deposited, in previous cycles, on the surface of the N95 and make easier ways for diffusion and penetration of more upstream particles to downstream in the next inhalation cycle. Another possible explanation could be due to the inevitable nature of the cyclic flow, where small portions of inhaled particles (those which penetrate at the relatively ultimate parts of the inhalation cycle) are returning back through the downstream line in the exhalation flow without being filtered by the high-efficiency particulate air (HEPA) filter installed on the manikin. Similarly, the exhaled air causes the dilution of both downstream and upstream flows. The dilution may contribute more with the upstream flow compared to downstream flow, since the exhaled air is purified with two filters (HEPA and N95) while the downstream flow is diluted by only one filter (HEPA). This may ultimately increase the amount of penetration for the "inhalation and exhalation" case. None of these phenomena however take place in the "inhalation only" set-up due to the one-way nature of the examined flow. Figure 3.5 summarizes the measured penetration for the MPPS range for all tested cyclic flows for both set-ups.

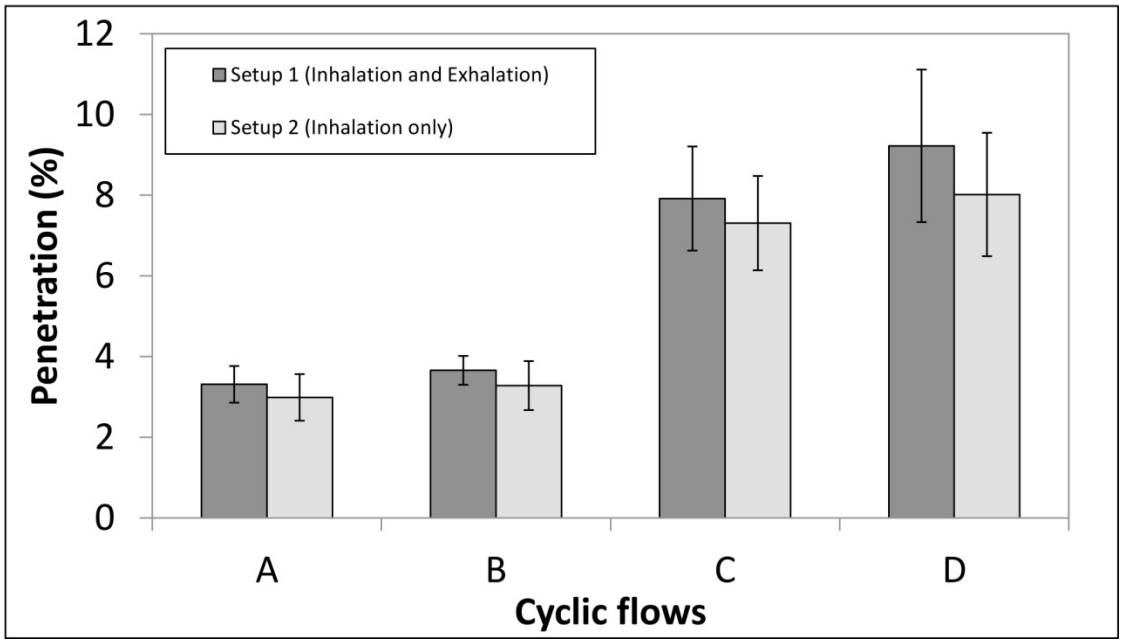

Figure 3.5 – Comparison of particle penetrations at the MPPS range for cyclic flows A, B, C and D, for both experimental set-ups

3.2 N95 FFRs Efficiency against UFPs under Cyclic and Constant Flows

The data reported in this section has been published in the Journal of Occupational and Environmental Hygiene (Bahloul *et al.* [84]).

3.2.1 Concentration Distributions

The challenge concentrations were obtained from polydispersed NaCl aerosols generated by a 6-jet Collison nebulizer (0.1 v/v NaCl solution). Figure 3.6 illustrates a typical upstream concentration distribution within the range of 10-205.4 nm for a cyclic flow with a PIF of 270 L/min (or 85 L/min as minute volume) for the five different test replicates done for this flow rate.

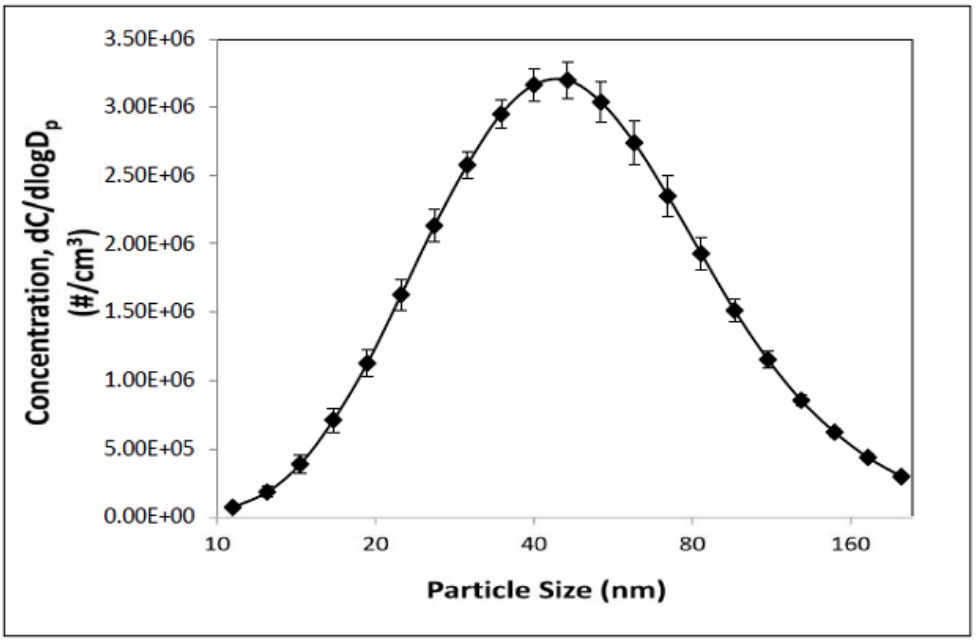

Figure 3.6 – Typical concentration distribution at N95 FFR upstream for the cyclic flow with 270 L/min as PIF

3.2.2 Particle Penetration for Constant and Cyclic Flows

The penetration curves for cyclic flows with PIFs of 135, 210, 270 and 360 L/min (groups G3 to G6 in table 2.2) are illustrated in figures 3.7, 3.8, 3.9, and 3.10, respectively (solid black lines). Each cyclic flow curve is accompanied by three other curves (dashed grey lines) corresponding to the penetration of particles under constant flows equivalent to the cyclic flow minute volume, MIF and PIF.

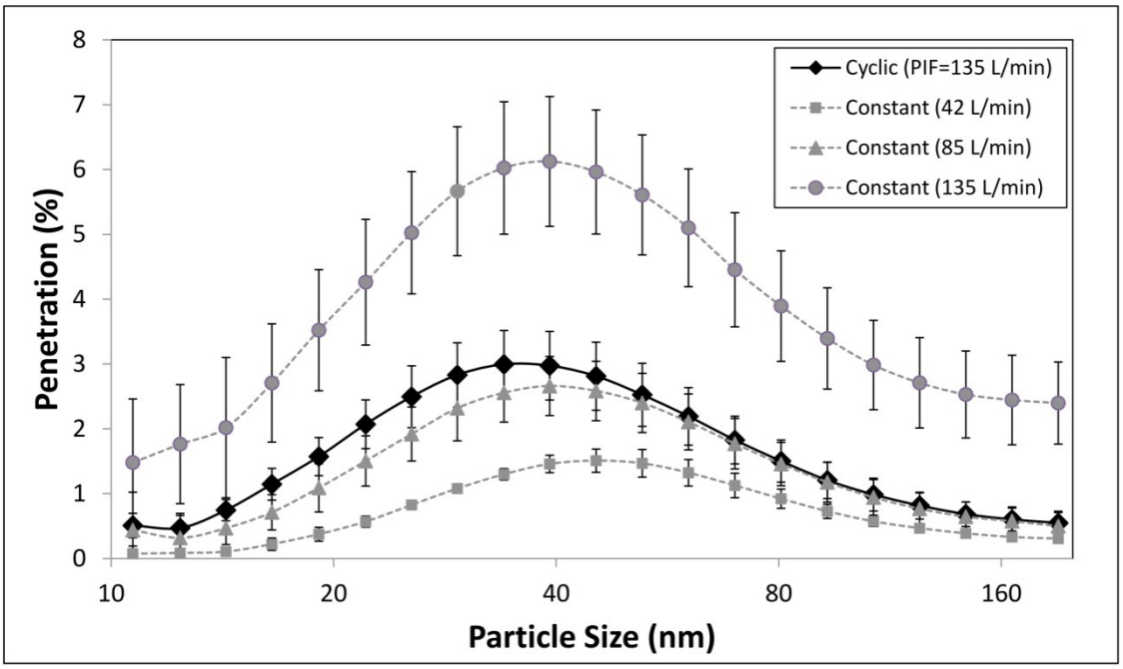

Figure 3.7 – Penetration of particles under one cyclic flow (minute volume: 42 L/min, MIF: 85 L/min, PIF: 135 L/min) and three constant flows of 42, 85 and 135 L/min

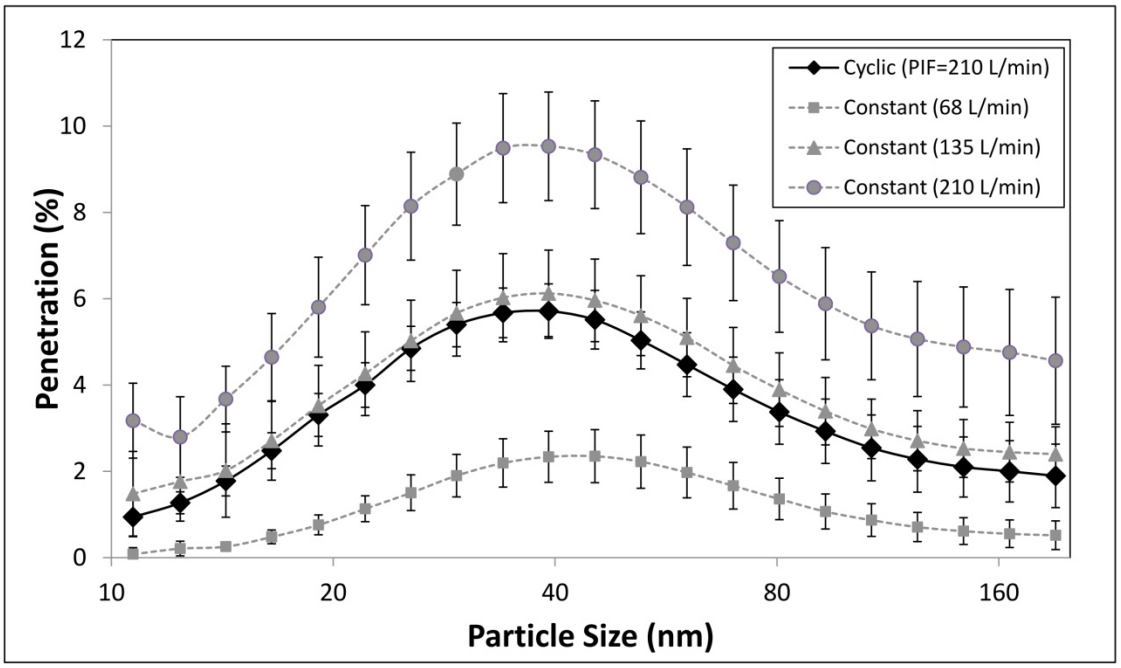

Figure 3.8 – Penetration of particles under one cyclic flow (minute volume: 68 L/min, MIF: 135 L/min, PIF: 210 L/min) and three constant flows of 68, 135 and 210 L/min

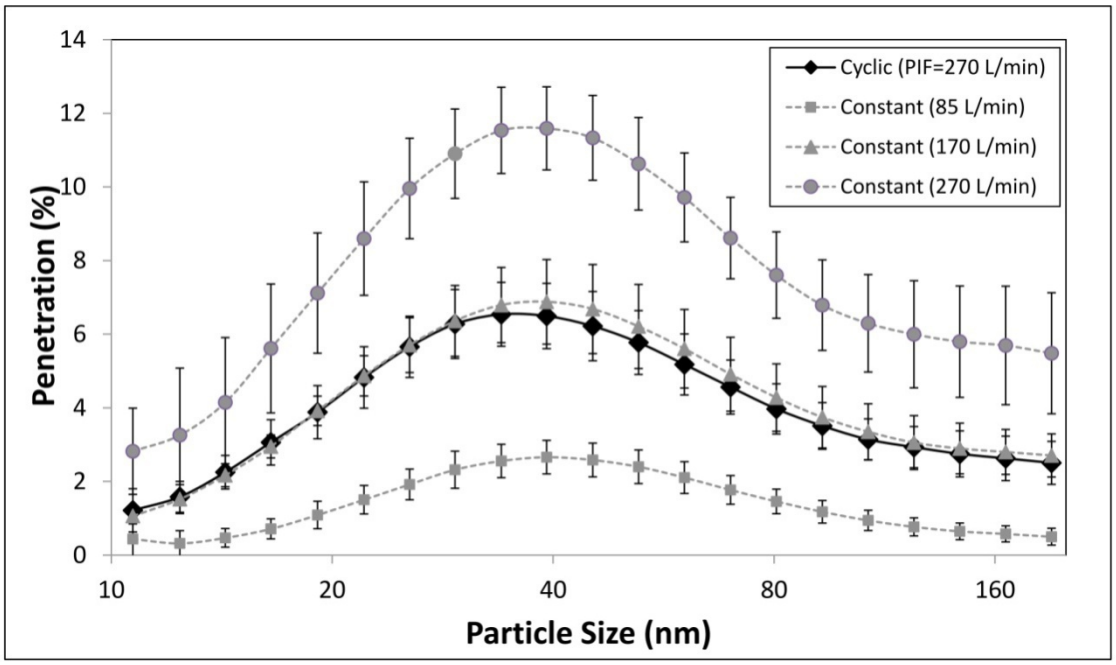

Figure 3.9 – Penetration of particles under one cyclic flow (minute volume: 85 L/min, MIF: 170 L/min, PIF: 270 L/min) and three constant flows of 85, 170 and 270 L/min

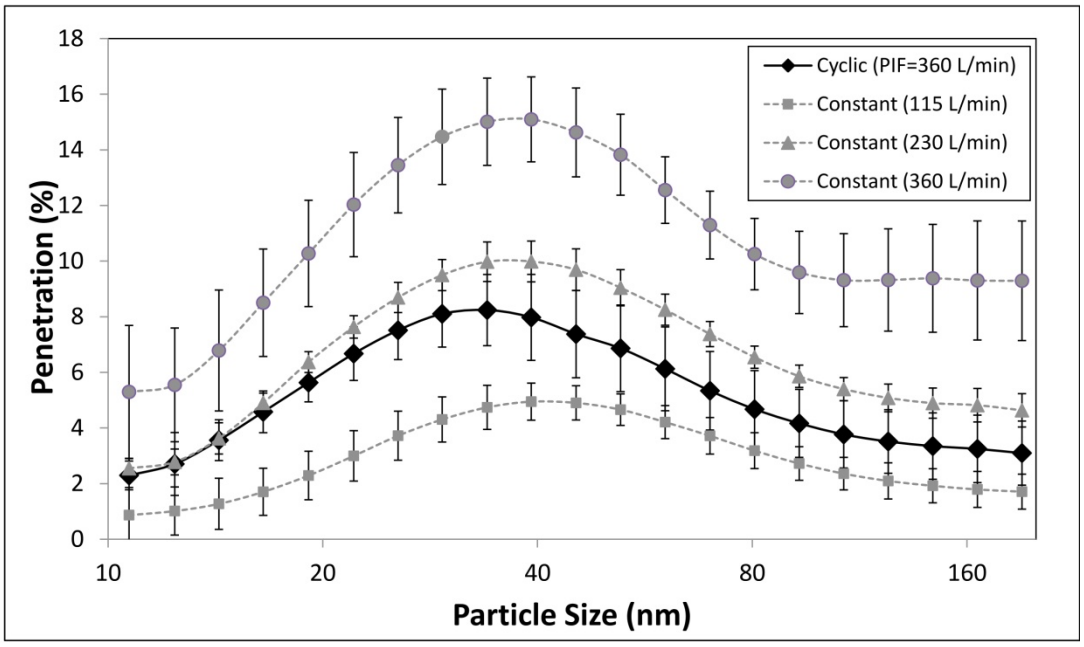

Figure 3.10 – Penetration of particles under one cyclic flow (minute volume: 115 L/min, MIF: 230 L/min, PIF: 360 L/min) and three constant flows of 115, 230 and 360 L/min

As shown in figures 3.7 to 3.10, and regardless of the magnitude of the selected cyclic or constant flows, particle penetration measured under cyclic flow was always higher than particle penetration measured under constant flow equivalent to the minute volume of the cyclic flow. For example, particle penetration at MPPS under the constant flow rate of 85 L/min reached 2.66 ± 0.46 %, while for the cyclic flow with the same flow rate as the minute volume (270 L/min as PIF), it reached 6.54 ± 0.87 % (figure 3.9 and table 3.3). This shows that the constant flow equal to the cyclic flow minute volume underestimates the penetration measured with the cyclic flow. On the other hand, since NIOSH selection is an 85 L/min constant flow as the minute volume for breathing under high workloads, it is necessary to verify the penetration with cyclic flow as well, due to the significant increase in penetration produced by the cyclic flow compared to the constant flow (equal to the minute volume of the cyclic flow). The lower particle penetration measured under constant flow (matching the cyclic flow minute volume) compared to the actual cyclic flow is consistent with earlier results [58,59,64,66]. The similarities observed among these findings (despite variations in the experimental set-ups and conditions) suggest that the lower particle penetration recorded for the constant flow (matching the cyclic flow minute volume) is independent of the set-up and conditions (such as flow magnitude, filter type, particle material, size and concentration distribution).

Table 3.3 – Summary of penetrations at MPPS for various constant and cyclic flows

	Penetration at MPPS (%)				MPPS (nm)			
Flow group	Cyclic flow (PIF)	Constant flow			Cyclic flow (PIF)	Constant flow		
		equal to cyclic minute volume	equal to cyclic MIF	equal to cyclic PIF		equal to cyclic minute volume	equal to cyclic MIF	equal to cyclic PIF
G1	1.55 ± 0.27 (68 L/min)	N/A	1.51 ± 0.18 (42 L/min)	2.35 ± 0.61 (68 L/min)	39.2	N/A	45.3	45.3
G2	2.53 ± 0.75 (105 L/min)	N/A	2.35 ± 0.61 (68 L/min)	N/A	39.2	N/A	45.3	N/A
G3 (fig. 3.7)	2.99 ± 0.52 (135 L/min)	1.51 ± 0.18 (42 L/min)	2.66 ± 0.46 (85 L/min)	6.12 ± 1.00 (135 L/min)	34.0	45.3	39.2	39.2
G4 (fig. 3.8)	5.71 ± 0.63 (210 L/min)	2.35 ± 0.61 (68 L/min)	6.12 ± 1.00 (135 L/min)	9.53 ± 1.26 (210 L/min)	39.2	45.3	39.2	39.2
G5 (fig. 3.9)	6.54 ± 0.87 (270 L/min)	2.66 ± 0.46 (85 L/min)	6.88 ± 1.15 (170 L/min)	11.59 ± 1.13 (270 L/min)	34.0	39.2	39.2	39.2
G6 (fig. 3.10)	8.24 ± 1.28 (360 L/min)	4.95 ± 0.67 (115 L/min)	9.99 ± 0.73 (230 L/min)	15.10 ± 1.53 (360 L/min)	34.0	39.2	39.2	39.2
G7	9.42 ± 1.62 (430 L/min)	6.12 ± 1.00 (135 L/min)	11.59 ± 1.13 (270 L/min)	N/A	34.0	39.2	39.2	N/A
G8	12.35± 1.14 (570 L/min)	N/A	15.10 ± 1.53 (360 L/min)	N/A	34.0	N/A	39.2	N/A

Compared to the minute volume, an inverse situation occurs when the penetration by the cyclic flow is compared with a constant flow equivalent to the PIF of the cyclic flow. For example, particle penetration values at MPPS, measured under a cyclic flow of 270 L/min as PIF and a constant flow having the same value, were 6.54 ± 0.87 and 11.59 ± 1.13 %, respectively (figure 3.9 and table 3.3). This shows that the selection of a constant flow equal to the PIF of the corresponding cyclic flow overestimates the penetration obtained by the cyclic flow. The latter is consistent with the results of Richardson *et al.*, Eshbaugh *et al.* and Wang *et al.*, despite the difference in the selection of a filter type, particle material and size range [60,64,66].

Unlike the minute volume and PIF, a constant flow equivalent to the MIF of the cyclic flow typically gives a better estimate of the penetration values when compared to the cyclic flow. For example, particle penetration values at MPPS, measured under a cyclic flow of 170 L/min as MIF and a constant flow having the same value, were 6.54 ± 0.87 and 6.88 ± 1.15 %, respectively (figure 3.9 and table 3.3). This cyclic flow (170 L/min as MIF) corresponds to the flow rate of the NIOSH certification (as the minute volume for this flow rate is 85 L/min). The particle penetration values obtained at MPPS for these flow rates demonstrate that instead of a constant flow equal to the minute volume of the cyclic flow, a constant flow equal to the MIF of the cyclic flow (double of minute volume) is a better estimator of penetration under cyclic flow. This case may, of course, not completely reflect the NIOSH's certification for filter penetration, due to their selection of 85 L/min as minute volume. Despite such a selection, it was shown in this study that a cyclic flow with an equivalent minute volume will result in significantly higher penetrations compared to its equivalent constant flow ($p<0.001$). In other words, using 85 L/min as the equivalent minute volume for a cyclic flow will result in an underestimation of the NIOSH test criteria (penetration at a constant flow of 85 L/min).

3.2.3 Particle Penetration at MPPS in Terms of Flow Magnitude and Pattern

Table 3.3 summarizes the maximal particle penetration values and the MPPS for all tested flow conditions (G1 to G8). Penetration values at the MPPS are also illustrated in figure 3.11. For the cyclic flows, three different curves present the results according to minute volume, MIF, and PIF. The cyclic flow curves corresponding to the PIF and the minute volume report only the data for groups G3 to G6; however, the cyclic flow curve corresponding to the MIF includes the data for all 8 groups. For both the cyclic and constant flow curves, an almost linear increase is observed with an increase in flow rate.

Figure 3.11 clearly illustrates that the constant flow equivalent to the MIF of the cyclic flow can best represent penetration values that can be obtained at MPPS (worst-case scenario) under the cyclic flow. The statistical analysis for comparisons between constant and cyclic flows using one-way ANOVA indicated that the difference between the flows in groups G1 to G5 (42 to 170 L/min) was not significant ($0.311<p<0.775$). However, for the last three flows (G6, G7 and G8; 230 to 360 L/min), the difference in the penetration measured at MPPS between the cyclic and constant flows was statistically significant ($0.012<p<0.039$).

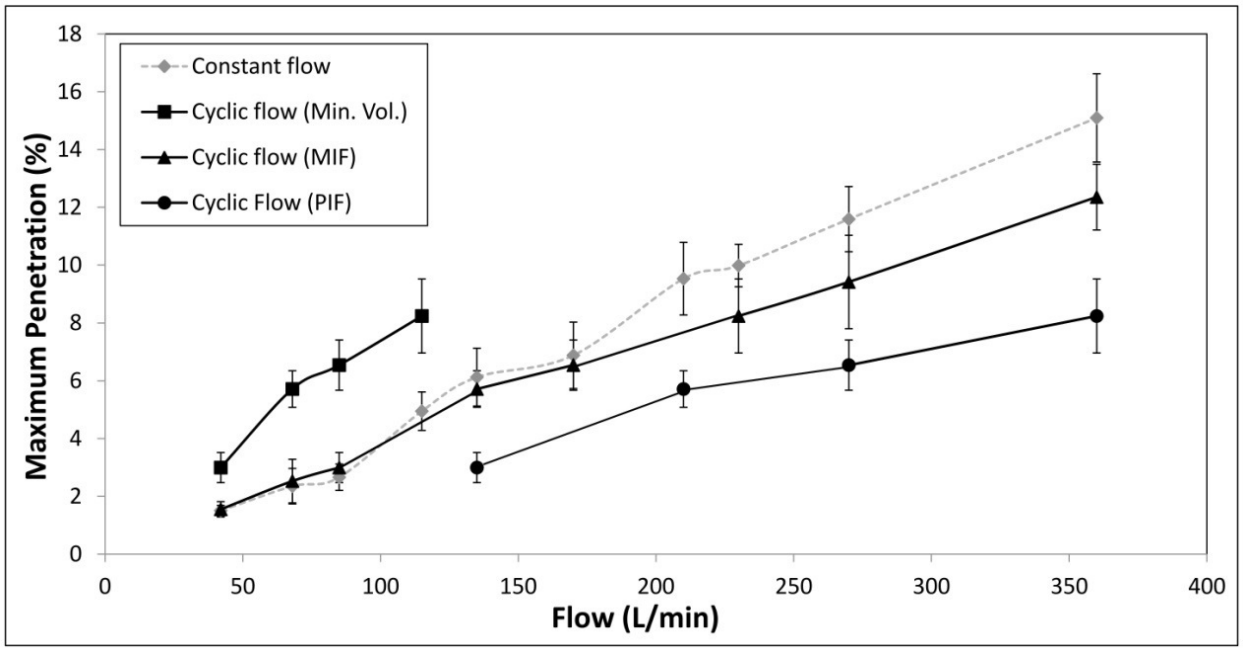

Figure 3.11 – Penetrations at MPPS in terms of constant and cyclic flows (indicated as minute volumes, MIFs or PIFs)

The results for the two-way ANOVA indicated a statistically significant difference in penetration at MPPS, as a result of both flow magnitude and flow pattern ($p<0.001$) and their interaction ($p=0.014$). The effective interaction between the two factors, namely flow magnitude and flow pattern, revealed that depending on the magnitude of the flows, penetration at MPPS for cyclic flow and constant flow (equal to cyclic MIF) could be equal or significantly different (higher for constant flows).

The findings of this study on the comparison of constant and cyclic flow impact on particle penetration are not always consistent with the results of Richardson *et al.*, Eshbaugh *et al.* and Wang *et al.* [60,64,66]. A constant flow equivalent to the cyclic MIF, in the current study, seems to give equal or higher penetration compared with the cyclic flow. This could be due to variations in the testing parameters such as the type and model of the test filter (one model of N95 FFRs), the type of particles (NaCl), and the experimental set-up (use of manikin). Unlike the results presented here, the results of Eshbaugh *et al.* and Richardson *et al.* are generalized for various types of N95 and P100 (FFRs and cartridges) and various particle materials (NaCl, DOP, PSL and Emery 3004) [60,64].

The findings of this study, on the other hand, showed more coherence with the results of Haruta *et al.* [61], since penetration under constant flows tended to exceed penetration under cyclic flow when the flow rate was increased. It should be noted that both studies used a manikin-based protocol, while Richardson *et al.* and Eshbaugh *et al.* did not use a manikin head to hold the filters [60,64]. Further theoretical research work is however required to have a better understanding of this process and of the influence of the different testing parameters on filter efficiency. Of course, in spite of the general similarity between the tendency of the results of this study and those of Haruta *et al.* [61], the difference of constant and cyclic flow penetration at the

MPPS was obvious for very high air flow rates (higher than selected values by Haruta *et al.* [61]). The difference in values could be attributed to the type of materials tested (NaCl versus PSL) and the type of filters used.

As observed in the results of the first objective, the MPPS channels for the tested constant and cyclic flows were located at 34.0, 39.2 or 45.3 nm size channels, showing the presence of electrostatic attraction in addition to diffusion and interception. The latter is consistent with several earlier studies carried out for N95 respirators [31–33,64,80,82]. The current results show that the MPPS tended to shift slightly towards larger sizes when the flow rate was lowered. For example, for constant flows, the MPPS was displaced from 39.2 to 45.3 nm from high flow rates (115 L/min and above) to lower flow rates (85 to 42 L/min). Such a tendency is mainly due to the fact that under lower flow rates the diffusion and electrostatic attraction mechanisms are enhanced, while interception is independent of the velocity [35]. This is consistent with both filtration theory and experimental results [27,33,34].

3.3 Particle Loading Time Effect on the Efficiency of N95 FFRs with Constant and Cyclic Flows under Varying RH Conditions

3.3.1 Penetration as a Function of Loading Time at 10 % RH

Figure 3.12 indicates typical upstream concentration percentages under different RH conditions for the loading time tests.

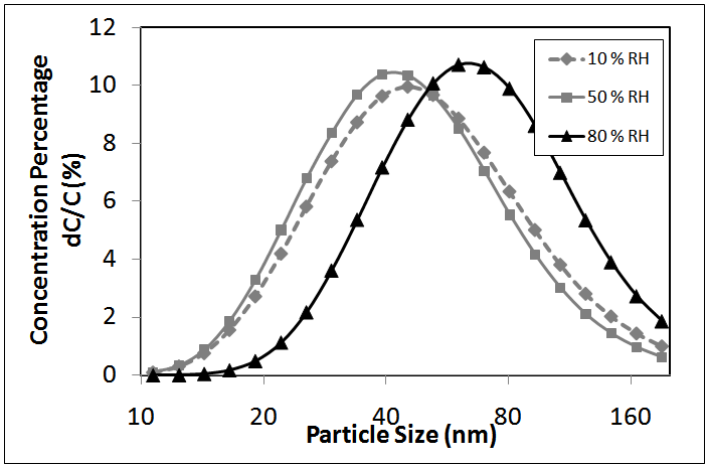

Figure 3.12 – Typical upstream concentration percentages for various RH conditions

Penetration, as well as the MPPS, varies in function of the loading time. Figures 3.13a, b and c report the changes in size distribution and MPPS for 10-205.4 nm polydispersed particles

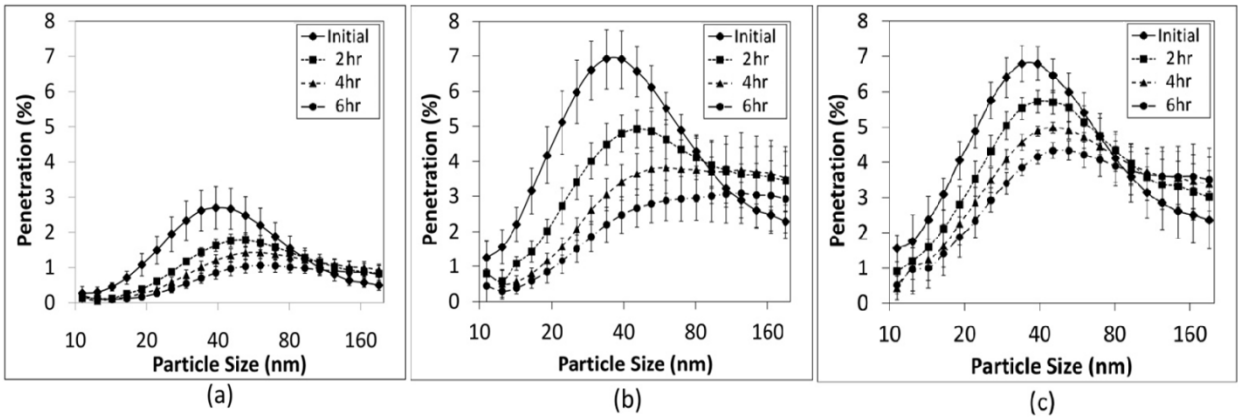

submitted to different constant flow rates, for loading times up to six hours in a 10 % RH.

Figure 3.13 – Particle penetration at different loading times, in a 10 % RH condition for a) a constant flow of 85 L/min, b) a constant flow of 170 L/min and c) a cyclic flow of 170 L/min as MIF

These plots show that the penetration for particles smaller than 80 nm (including MPPS) has been reduced with the loading time under the cyclic (170 L/min as MIF) and constant flow rates (85 and 170 L/min) at a 10 % RH. For instance, penetrations at MPPS under 85 L/min constant flow rate were reported as 2.70 ± 0.60, 1.78 ± 0.21, 1.42 ± 0.17 and 1.06 ± 0.19 % at the initial loading time, 2, 4 and 6 hours, respectively. For particles which are larger than 80 nm, this trend was partially reversed. The MPPS also shifted from 39.2 nm to 60.4 nm from the initial to the final state of loading time (6 hours). The change in penetration at MPPS, in terms of loading time, was found to be statistically significant ($p<0.001$). Similar results were obtained for the constant flow rate of 170 L/min where the penetration was significantly reduced ($p<0.001$) by using a one-way ANOVA test. In this specific case, the penetration at MPPS was reduced from 6.92 ± 0.85 to 3.08 ± 0.84 % for the initial and final stages of the loading time (6 hours). The MPPS was shifted from 34.0 to larger sizes. By increasing the flow rate, the shift of the MPPS towards larger sizes was found to be substantially more important. It was also observed that, for the final stage of the loading test (6 hours), the location of the MPPS was not sharply defined since penetrations were almost equal for various sizes of particles close to the MPPS (figure 3.13b). For the cyclic flow, penetration of smaller particles (mostly <80 nm) was found to be significantly decreased by increasing the loading time ($p<0.001$). Penetrations at MPPS for the initial and the 6-hour stages of loading time for this flow rate was reported as 6.80 ± 0.52 and 4.33 ± 0.28 %, respectively. The shift in the MPPS was from 34.0 to 52.3 nm for the initial and final stages of loading and it was found to be less obvious compared to constant flow rates.

The reduction of the penetration in the nanometer range and the shift in the MPPS towards larger particle sizes could be possibly explained by the enhancement of the diffusion mechanism, as the filter is loaded with more particles. With such a phenomenon, there is less space for new particles to diffuse through the filter media and the probability of collisions between particles and filter fibers (due to random Brownian motion) is increased. It is important to note that all the above findings are interpreted based on experimental data and only for one model of N95 FFRs. The reduction in penetration (at nanometer sizes) with loading time is consistent with the results of previous works [34,78].

For larger size particles (usually more than 100 nm), a reverse tendency in penetration was observed in comparison with nanometer sizes. For constant flow rates of 85 L/min and 170 L/min, penetrations at loading time stages of 2 and 4 hours were found to be slightly higher compared with the initial stage. For the 6 hour stage, however, a slight decrease in penetration was observed, compared to the 4 hour stage. This reduction could be attributed to the formation of dendrites which inhibit more particle penetration as suggested in the literature [45]. For the cyclic flow rate, on the other hand, penetration of large particles (>100 nm) was continuously increased with loading time. The increase in penetration for larger size particles suggests that the electrostatic attraction has been reduced over loading time [45,79].

3.3.2 Penetration as a Function of Loading Time at 50 and 80 % RH

When the figure 3.13 is compared to figures 3.14 to 3.15, it shows that when the RH increases from 10 to 50 or to 80 %, the filter behaves differently. In general, penetration within the tested particle size range, at 50 and 80 % RH, was found to increase rather than decrease. At 50% RH, penetrations at the MPPS at the initial and final (6 hours) loading time stages increased from 3.47 ± 0.56 to 4.57 ± 0.58 % for the constant flow rate of 85 L/min, and from 7.79 ± 0.88 to 9.44 ± 0.82 % for the constant flow rate of 170 L/min (see figures 3.14a,b). This change in penetration at the MPPS, in terms of loading time, was statistically significant (p=0.044) for 170 L/min, and close to significant (p=0.069) for 85 L/min. The MPPS also shifted for both flow rates (from 29.4 to 39.2 nm for the 85 L/min flow and from 25.5 to 34.0 nm for the 170 L/min flow). For the cyclic flow (see figure 3.19), the penetration at the MPPS changed from 7.44 ± 0.92 to 7.89 ± 0.86 %, which was, in this case, not statistically significant (p=0.87). However, the MPPS shifted slightly from 29.4 to 34.0 nm.

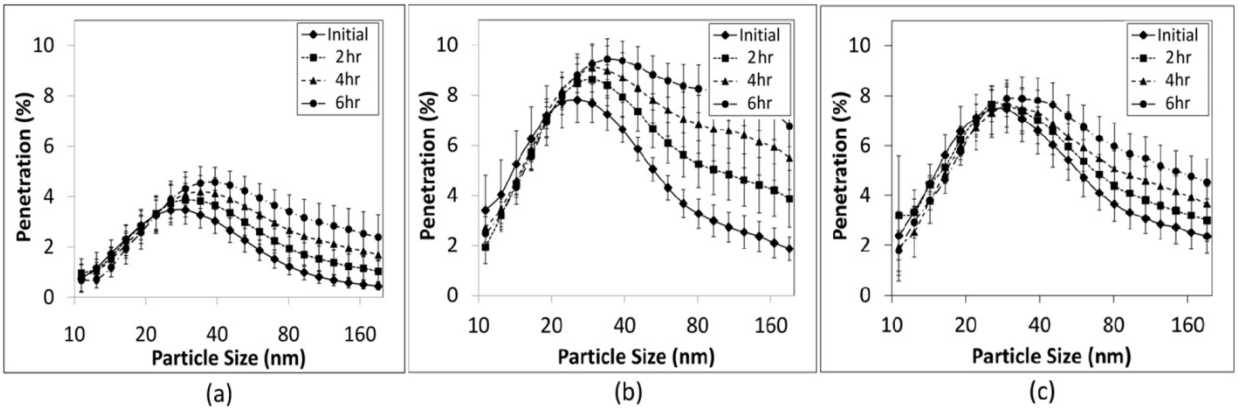

Figure 3.14 – Particle penetration at different loading times, in a 50 % RH condition for a) constant flow of 85 L/min; b) constant flow of 170 L/min; and, c) cyclic flow of 170 L/min as MIF

At high RH (80 %), loading time effect on penetration was similar to the one observed at 50 % RH. For instance, penetrations at MPPS at a 6-hour loading time for the 85 and 170 L/min constant flow rates increased from 3.63 ± 0.65 to 5.21 ± 0.63 % and from 8.49 ± 1.18 to 11.10 ± 1.26 %, respectively (figures 3.15a,b). The change in the penetration at the MPPS over time was statistically significant for both 85 L/min (p=0.007) and 170 L/min (p=0.025) flow rates. The MPPS also increased slightly for both flow rates (39.2 to 45.3 nm for 85 L/min and 34.0 to 45.3 nm for 170 L/min). For cyclic flow, penetration at MPPS varied from 8.15 ± 1.03 to 9.05 ± 1.12 % (figure 3.15c), which was found to be insignificant (p=0.546). In fact, a substantial increase in penetration for cyclic flow, under high humidity levels (50 and 80 %), could be observed only with particles which are larger than the MPPS (figures 3.15b,c).

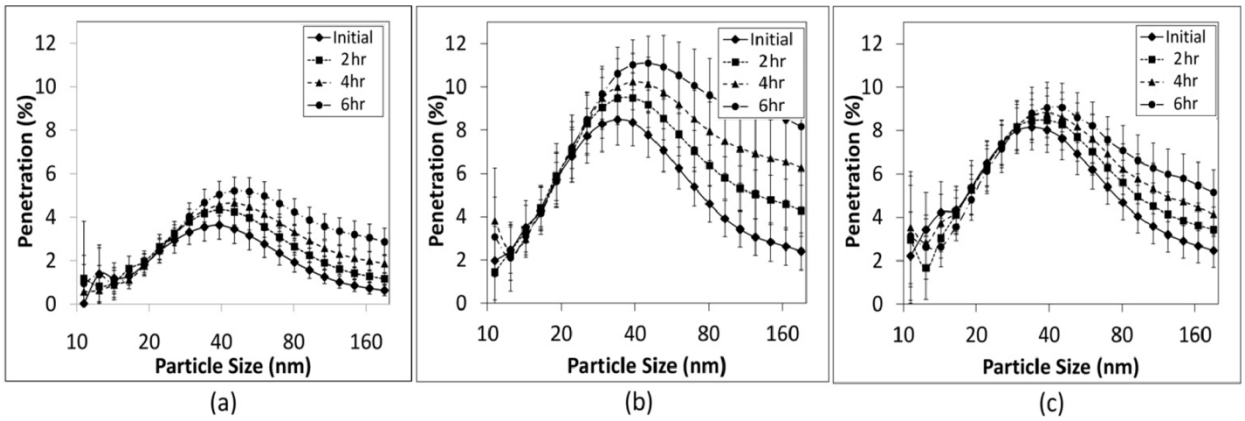

Figure 3.15 – Particle penetration at different loading times, in an 80 % RH condition for a) constant flow of 85 L/min; b) constant flow of 170 L/min; and, c) cyclic flow of 170 L/min as MIF

As suggested by Ikezaki *et al.* [85] and Lowkis and Motyl [86], the enhancement in penetration over time at high RH levels could be mainly due to the loss of surface electrostatic potential when the filter is exposed to humid air for a long period of time. Accordingly, this phenomenon could be potentially accompanied with an enhancement in penetration of large particles through the filter. The increase in penetration in this study, when the filter is exposed to humidity for long periods (compared to the case of "as-received"), is in agreement with earlier findings [80,31,79]. There could also be an impact of high RH on NaCl particles, which could affect particle penetration.

3.3.3 Comparison of Constant and Cyclic Flow Penetrations at Initial and Final Stages of Loading Time

From figures 3.13a,c (10 % RH), it can be concluded that the penetration under a constant flow rate of 85 L/min equivalent to minute volume of the cyclic flow is significantly less than the penetration under this cyclic flow ($p<0.001$), whether it is at the initial or at the final stage of the loading period (after 6 hours). This indicates that, regardless of the period for which the respirator is exposed by the particles, the constant flow equivalent to cyclic flow minute volume does not accurately represent the efficiency of the filters under cyclic flow (which is more representative of the breathing pattern in humans). This has also been reported in previous studies found in the literature [58,59,64,66].

Unlike minute volume, a constant flow equal to the MIF of the cyclic flow can properly represent the penetration obtained by cyclic flow, since penetration curves were almost identical ($p=0.793$) for initial loading time (see initial penetration curves in figures 3.13b,c). This is consistent with the results of Haruta *et al.* [61] comparing constant and cyclic flow with a MIF rate of 85 L/min. On the other hand, at the final stage (after 6 hours), penetrations under cyclic flow for a wide range of particles (normally within 20-80 nm) was found to be significantly in excess ($p<0.038$) with the final stage penetration measured for constant flow (equal to cyclic MIF) (see 6 hour penetration curves in figures 3.13b,c). Such a difference in constant and cyclic flow penetration at the final stage of loading suggests that the rate of particle loading could be

less under cyclic flow compared to constant flow. One possible explanation for this phenomenon is that the exposure time, for cyclic flow, is limited to inhalation cycles only (which represent half of the respiration cycles). While for constant flow, the filter is exposed to the particles throughout the whole period of the exposure time. Therefore particle loading takes place at a higher rate for the constant flow condition. The increase in cyclic flow penetration compared with constant flow equal to MIF is consistent with the results of Wang *et al.* and Eshbaugh *et al.* [64,66].

The summary of the results from the two-way ANOVA indicated that both loading time and flow pattern (cyclic or constant equal to cyclic flow MIF) are significant parameters in variations of the penetration at the MPPS ($p<0.001$). The analysis indicated almost a significant interaction between the two factor variables ($p=0.051$). The interaction between loading time and flow pattern shows that, in different loading time stages, equal or different penetrations at MPPS could take place by constant and cyclic flows.

At 50 and 80 % RH, penetration of particles (usually at the MPPS and larger sizes), at the final loading time stage, was found to be significantly greater with constant flow than with cyclic flow ($0.003<p<0.026$), despite almost equal penetrations recorded at the initial stage. In fact, the rate of increase in penetration (as a function of loading time for 50 and 80 % RH conditions) was observed to be higher for constant than for cyclic flows. Two separate two-way ANOVAs were performed, one at 50 and one at 80 % RH to investigate the flow pattern (constant vs. cyclic) and loading time effect on maximum penetration. At 50 % RH, for instance, it was shown that the impact of the flow pattern, cyclic or constant, is significant on penetration ($p<0.001$). Loading time impact was found to be close to significant ($p=0.066$). However, no significant interaction was found between loading time and flow pattern ($p=0.38$). The two-way ANOVA, at 80 % RH, also indicated that penetration at MPPS is significantly influenced by loading time ($p=0.014$) and flow pattern ($p=0.003$). The interaction between the two factors was, however, not statistically significant ($p=0.42$).

3.4 Limitations and Future Works

Despite the findings presented in this study, there are several limitations with the current research. These limitations could lead to future research orientations and can be stratified in different categories:

1. Reported findings of this research are limited to only one model of FFRs. In fact, because of the specific geometrical and physical characteristics of different filter types (FFR, cartridges, etc.) and filter materials (N-series, R-series, P-series, etc.), filter penetration could substantially vary among different types, models, suppliers, and materials of filters. Also, the current study involved only one type of generated aerosols (NaCl). Other aerosol types (DOP, PSL, etc.) could potentially have a different impact on the efficiency of the filters, due to their difference in physical and chemical properties. Thus, measuring particle penetration for various types of filters and aerosols could be the scope of future work to address the impact of various conditions on the efficiency of filtration devices.

2. Even though the measurement of particle penetration is beneficiary to assess filter efficiency in capturing UFPs, it should be noted that there is still significant knowledge gaps when one considers the real usage situation where face-seal leaks are likely to be present. Indeed, in real life, filters are not sealed to the face. Therefore, sealed filters on manikin do represent the most efficient scenario. Recent studies have demonstrated that particle penetration due to face-seal leakage can be very significant. For instance, Grinshpun *et al.* [63] found out that the amount of 40 nm particles penetrating through face-seal leakage was, on average, seven times larger than the quantity penetrating through the filter medium. Similarly, other studies investigated particle penetration through face-seal leaks, compared the results with those obtained with sealed filters [7,65,62] and found out that the total inward leakage through the filter is higher compared to the filter penetration. Therefore, it is imperative that the influence of face-seal leakage be investigated, in addition to other experimental parameters, in future works.

3. The results presented in the current study regarding the loading effect are limited to particle penetration measurements. This is a rather simplified method for measuring the penetration of particles through filters. A quantitative approach, which consists of measuring particle penetration in terms of the mass of particles deposited on the surface of the filters, would represent an appropriate way of validating the results emerging from the comparison between the cyclic and constant flows. Such investigations could be the scope of future studies aiming at assessing the loading effect with a more comprehensive approach. Also, the number of flow rates performed under cyclic and constant flows for the loading time tests was limited. More data could thus be collected through these future research projects.

4. All the cyclic flows used in this study followed a sinusoidal pattern and all selected constant flows were based on specific values expressed as the minute volume, MIF and PIF. In reality, human breathing does not follow a perfect sinusoidal pattern. Different working efforts as well as workers' personal health conditions could be associated with different respiratory flow patterns, resulting in different particle penetration measurements. For instance, Wang *et al.* [66] found that, with a same minute volume (50 L/min), penetration under a sinusoidal flow was higher than under a trapezoidal flow, but less than under an exponential flow, for 300 nm

particles. Future work could therefore assess the impact of flow patterns on the efficiency of respiratory filters for various particles and flow rates.

5. This study was strictly experimental. A comprehensive theoretical approach using the single-fiber theory for the case of the N95 FFR would be a beneficial complement to the current study. A theoretical approach will help obtain a better understanding of the filtration mechanisms, potentially identifying their individual contribution to the overall filtration phenomena. The development of a predictive theoretical model to assess the effectiveness of the filters could also be helpful in understanding how the main parameters are affecting filtration efficiency and in supporting the development of more efficient respirators.

4 CONCLUSION

This study evaluated the efficiency of one model of N95 filtering facepiece respirators (FFR) challenged with polydispersed NaCl particles under cyclic and constant flows. Cyclic flow patterns and polydispersed aerosols were used for simulating working conditions. The aim was to identify which constant flow better correlates with the N95 FFRs efficiency measured under cyclic flows simulating real breathing situations.

The contributions of breathing frequency and peak inhalation flow (PIF) were first investigated under constant flow with two different experimental set-ups by considering “inhalation and exhalation” and “inhalation only” conditions. Results showed that PIF has a substantial significant effect on ultrafine particles (UFP) penetration while the impact of breathing frequency was limited. The experimental set-up with simulating “inhalation and exhalation” showed no significant difference in penetration when compared to the set-up simulating “inhalation only”. Therefore, the “inhalation only” set-up was used in the remaining parts of the study.

Comparisons of particle penetration measured under constant and cyclic flows were assessed for a wide range of flow rates. It was found that using a constant flow equal to the mean inhalation flow (MIF) provides a better estimate of the particle penetration for the cyclic flow than using a constant equal to either the PIF or the minute volume.

Particle loading effects were investigated for both constant and cyclic flows. Results showed that the loading time has a significant impact on particle penetration through N95 FFRs. For 10 % relative humidity (RH), penetration of smaller sizes (usually <100 nm) including the most penetrating particle size (MPPS) significantly dropped as the filter long-term exposure to the challenge particles increased. A distinct shift in the MPPS towards larger particles was also observed, with loading time. For 50 and 80 % RH, however, an almost reverse trend in penetration changes was observed due to the general increase of penetration (usually at MPPS and for larger sizes), in terms of loading time. The comparison between the cyclic and constant flows revealed that, in terms of loading time, a constant flow could not necessarily predict the penetration under the cyclic flow for long-term exposures.

Finally, the report suggests a series of potential future research orientations required to better understand the filter efficiency behaviour of FFRs against nanoparticles (NPs) and UFPs. First, further work is needed to validate the present results for other FFRs, the mostly used in working places in Quebec. Second, the impact of other influencing parameters with the use of N95 and other FFRs, such as mass of aerosol loaded, flow patterns and particle face-seal leakage could be defined as future research paths. Since the inhalation flow rate depends of both workload and human subject, obtaining the characteristic FFR efficiency curve, in term of flow rate, could be the scope of future research to provide a better optimal use of FFR according to each flow rate situation.

REFERENCES

[1] G. Oberdörster, E. Oberdörster, and J. Oberdörster, “Nanotoxicology: an emerging discipline evolving from studies of ultrafine particles”. *Environmental Health Perspectives*, vol. 113, no. 7, pp. 823–839, 2005.

[2] R. J. Aitken, K. S. Creely, C. L. Tran, and G. Britain, "Nanoparticles: An occupational hygiene review". HSE Books, 2004.

[3] M. J. Hull and J. L. Abraham, “Aluminum welding fume-induced pneumoconiosis” *Human Pathology*, vol. 33, no. 8, pp. 819–825, 2002.

[4] J. H. Vincent and C. F. Clement, “Ultrafine particles in workplace atmospheres” *Philosophical Transactions of the Royal Society A*, vol. 358, no. 1775, pp. 2673–2682, 2000.

[5] E.C. Teague, “Responsible Development of Nanotechnology.” National Nanotechnology Initiative Meeting, National Nanotechnology Initiative, 29 p., April 2, 2004.

[6] ISO/TS, Nanotechnologies — Terminology and Definitions for Nano-Objects—Nanoparticle, Nanofibre and Nanoplate. Geneva, Switzerland: International Standards Organization.”

[7] S. Rengasamy and B. C. Eimer, “Nanoparticle penetration through filter media and leakage through face seal interface of N95 filtering facepiece respirators” *Annals of Occupational Hygiene*, vol. 56, no. 5, pp. 568–580, 2012.

[8] S. Rengasamy, W. P. King, B. C. Eimer, and R. E. Shaffer, “Filtration performance of NIOSH-approved N95 and P100 filtering facepiece respirators against 4 to 30 nanometer-size nanoparticles” *Journal of Occupational and Environmental Hygiene*, vol. 5, no. 9, pp. 556–564, 2008.

[9] C. Ostiguy, B. Soucy, G. Lapointe, C. Woods, and L. Ménard, “Health Effects of Nanoparticles-Second Edition.” Studies and Research Projects / Report R-589, Montreal, IRSST, 2008. Available online at http://www.irsst.qc.ca/media/documents/PubIRSST/R-589.pdf [Accessed on March 12, 2015].

[10] A. D. Maynard and E. D. Kuempel, “Airborne nanostructured particles and occupational health” *Journal of Nanoparticle Research*, vol. 7, no. 6, pp. 587–614, 2005.

[11] J. D. Byrne and J. A. Baugh, “The significance of nanoparticles in particle-induced pulmonary fibrosis” *McGill Journal of Medicine*, vol. 11, no. 1, p. 43, 2008.

[12] G. Oberdörster, Z. Sharp, V. Atudorei, A. Elder, R. Gelein, A. Lunts, W. Kreyling, and C. Cox, “Extrapulmonary translocation of ultrafine carbon particles following whole-body inhalation exposure of rats” *Journal of Toxicology and Environmental Health A*, vol. 65, no. 20, pp. 1531–1543, 2002.

[13] G. Oberdörster, Z. Sharp, V. Atudorei, A. Elder, R. Gelein, W. Kreyling, and C. Cox, “Translocation of inhaled ultrafine particles to the brain” *Inhalation Toxicology*, vol. 16, no. 6–7, pp. 437–445, 2004.

[14] M. Semmler, J. Seitz, F. Erbe, P. Mayer, J. Heyder, G. Oberdörster, and W. G. Kreyling, "Long-term clearance kinetics of inhaled ultrafine insoluble iridium particles from the rat lung, including transient translocation into secondary organs" *Inhalation Toxicology*, vol. 16, no. 6–7, pp. 453–459, 2004.

[15] A. D. Maynard and R. J. Aitken, "Assessing exposure to airborne nanomaterials: Current abilities and future requirements" *Nanotoxicology*, vol. 1, no. 1, pp. 26–41, 2007.

[16] A. Nel, T. Xia, L. Mädler, and N. Li, "Toxic potential of materials at the nanolevel." *Science*, vol. 311, no. 5761, pp. 622–627, 2006.

[17] S. P. Faux, C. L. Tran, B. G. Miller, A. D. Jones, C. Monteiller, and K. Donaldson, "In vitro determinants of particulate toxicity: the dose-metric for poorly soluble dusts" Institute of Occupational Medicine, Research Report for the Health and Safety Executive, 2003. Available online at http://www.hse.gov.uk/research/rrpdf/rr154.pdf [Accessed on March 12, 2015].

[18] C. L. Tran, D. Buchanan, R. T. Cullen, A. Searl, A. D. Jones, and K. Donaldson, "Inhalation of poorly soluble particles. II. Influence of particle surface area on inflammation and clearance" *Inhalation Toxicology*, vol. 12, no. 12, pp. 1113–1126, 2000.

[19] A. Churg, "Particle Uptake by Epithelial Cells. In Gehr, P., Heyder, J., Editors. Particle-Lung Interactions." New York: Marcel Dekker. pp. 401–435. ISBN 0-8247-9891-0.

[20] G. Oberdörster, "Toxicology of ultrafine particles: in vivo studies" *Philosophical Transactions of the Royal Society A*, vol. 358, no. 1775, pp. 2719–2740, 2000.

[21] K. Donaldson, V. Stone, A. Clouter, L. Renwick, and W. MacNee, "Ultrafine particles" *Occupational and Environmental Medicine*, vol. 58, no. 3, pp. 211–216, 2001.

[22] G. Oberdörster, J. N. Finkelstein, C. Johnston, R. Gelein, C. Cox, R. Baggs, and A. C. Elder, "Acute pulmonary effects of ultrafine particles in rats and mice" *Research Report Health Effect Institute*, no. 96, pp. 5–74, 2000.

[23] P. Penttinen, K. L. Timonen, P. Tiittanen, A. Mirme, J. Ruuskanen, and J. Pekkanen, "Ultrafine particles in urban air and respiratory health among adult asthmatics" *European Respiratory Journal*, vol. 17, no. 3, pp. 428–435, 2001.

[24] H.-E. Wichmann, C. Spix, T. Tuch, G. Wölke, A. Peters, J. Heinrich, W. G. Kreyling, and J. Heyder, "Daily mortality and fine and ultrafine particles in Erfurt, Germany part I: role of particle number and particle mass" *Research Report Health Effect Institute*, no. 98, pp. 5–86, 2000.

[25] C. Ostiguy, B. Roberge, C. Woods, and B. Soucy, "Engineered Nanoparticles: Current Knowledge about Occupational Health and Safety Risks and Prevention Measures - Second Edition." Studies and Research Projects / Report R-656, Montreal, IRSST, 2010. Available online at http://www.irsst.qc.ca/media/documents/PubIRSST/R-656.pdf [Accessed on March 12, 2015].

[26] European Commission (2004). Nanotechnologies: A Preliminary Risk Analysis on the Basis of a Workshop Organised in Brussels on 1-2 March 2004 by the Health and Consumer Protection Directorate General of the European Commission". Available online at http://ec.europa.eu/health/ph_risk/documents/ev_20040301_en.pdf [Accessed on March 12, 2015].

[27] R. Mostofi, B. Wang, F. Haghighat, A. Bahloul, and J. Lara, "Performance of Mechanical Filters and Respirators for Capturing Nanoparticles – Limitations and Future Direction" *Industrial Health*, vol. 48, no. 3, pp. 296–304, 2010.

[28] C.-C. Chen and S.-H. Huang, "The effects of particle charge on the performance of a filtering facepiece" *American Industrial Hygiene Association Journal*, vol. 59, no. 4, pp. 227–233, 1998.

[29] S. Rengasamy, A. Miller, and B. C. Eimer, "Evaluation of the filtration performance of NIOSH-approved N95 filtering facepiece respirators by photometric and number-based test methods" *Journal of Occupational and Environmental Hygiene*, vol. 8, no. 1, pp. 23–30, 2011.

[30] "NIOSH. (1995) Respiratory protection devices. Title 42, Code of Federal regulation, Part 84. Washington, DC: U.S. Government Printing Office, Office of the Federal Register" pp. 30335–30398.

[31] S. B. Martin Jr and E. S. Moyer, "Electrostatic respirator filter media: filter efficiency and most penetrating particle size effects" *Applied Occupational and Environmental Hygiene*, vol. 15, no. 8, pp. 609–617, 2000.

[32] A. Balazy, M. Toivola, T. Reponen, A. Podgórski, A. Zimmer, and S. A. Grinshpun, "Manikin-based performance evaluation of N95 filtering-facepiece respirators challenged with nanoparticles" *Annals of Occupational Hygiene*, vol. 50, no. 3, pp. 259–269, 2006.

[33] R. M. Eninger, T. Honda, A. Adhikari, H. Heinonen-Tanski, T. Reponen, and S. A. Grinshpun, "Filter performance of N99 and N95 facepiece respirators against viruses and ultrafine particles" *Annals of Occupational Hygiene*, vol. 52, no. 5, pp. 385–396, 2008.

[34] R. Mostofi, A. Bahloul, J. Lara, B. Wang, Y. Cloutier, and F. Haghighat, "Investigation of potential affecting factors on performance of N95 respirator" *Journal of the International Society for Respiratory Protection*, vol. 28, no. 1, pp. 26–39, 2011.

[35] W. C. Hinds, "Aerosol technology: properties, behavior, and measurement of airborne particles" John Wiley & Sons, 2012.

[36] F. Haghighat, A. Bahloul, J. Lara, R. Mostofi, and A. Mahdavi, "Development of a Procedure to Measure the Effectiveness of N95 Respirator Filters against Nanoparticles" Studies and Research Projects / Report R-754, Montreal, IRSST 2012. Available online at http://www.irsst.qc.ca/media/documents/PubIRSST/R-754.pdf [Accessed on March 12, 2015].

[37] L. Janssen, "Principles of physiology and respirator performance" *Occupational Health and Safety*, vol. 72, no. 6, pp. 73–81, 2003.

[38] R. C. Brown, D. Wake, R. Gray, D. B. Blackford, and G. J. Bostock, “Effect of industrial aerosols on the performance of electrically charged filter material” *Annals of Occupational Hygiene*, vol. 32, no. 3, pp. 271–294, 1988.

[39] R. A. Fjeld and T. M. Owens, “The effect of particle charge on penetration in an electret filter” *Industry Application IEEE Transactions*, vol. 24, no. 4, pp. 725–731, 1988.

[40] L. L. Janssen, J. O. Bidwell, H. E. Mullins, and T. J. Nelson, “Efficiency of degraded electret filters: Part I. Laboratory testing against NaCl and DOP before and after exposure to workplace aerosols” *Journal of the International Society for Respiratory Protection*, vol. 20, pp. 71–80, 2003.

[41] S.-H. Huang, C.-W. Chen, C.-P. Chang, C.-Y. Lai, and C.-C. Chen, “Penetration of 4.5 nm to aerosol particles through fibrous filters” *Journal of Aerosol Science*, vol. 38, no. 7, pp. 719–727, 2007.

[42] Y.-W. Oh, K.-J. Jeon, A.-I. Jung, and Y.-W. Jung, “A simulation study on the collection of submicron particles in a unipolar charged fiber” *Aerosol Science and Technology*, vol. 36, no. 5, pp. 573–582, 2002.

[43] A. Balazy, M. Toivola, A. Adhikari, S. K. Sivasubramani, T. Reponen, and S. A. Grinshpun, “Do N95 respirators provide 95% protection level against airborne viruses, and how adequate are surgical masks?” *American Journal of Infection Control.*, vol. 34, no. 2, pp. 51–57, 2006.

[44] Y. Qian, K. Willeke, S. A. Grinshpun, J. Donnelly, and C. C. Coffey, “Performance of N95 respirators: Filtration efficiency for airborne microbial and inert particles” *American Industrial Hygiene Association journa.*, vol. 59, no. 2, pp. 128–132, 1998.

[45] C.-S. Wang, “Electrostatic forces in fibrous filters—a review” *Powder Technology*, vol. 118, no. 1, pp. 166–170, 2001.

[46] C. S. Kim, L. Bao, K. Okuyama, M. Shimada, and H. Niinuma, “Filtration efficiency of a fibrous filter for nanoparticles” *Journal of Nanoparticle Research*, vol. 8, no. 2, pp. 215–221, 2006.

[47] S. Yang and G. W. Lee, “Filtration characteristics of a fibrous filter pretreated with anionic surfactants for monodisperse solid aerosols” *Journal of Aerosol Science*, vol. 36, no. 4, pp. 419–437, 2005.

[48] S. Yang, W.-M. G. Lee, H.-L. Huang, Y.-C. Huang, C.-H. Luo, C.-C. Wu, and K.-P. Yu, “Aerosol penetration properties of an electret filter with submicron aerosols with various operating factors” *Journal of Environmental Science and Health Part A*, vol. 42, no. 1, pp. 51–57, 2007.

[49] S. C. Kim, M. S. Harrington, and D. Y. Pui, “Experimental study of nanoparticles penetration through commercial filter media” *Journal of Nanoparticle Research*, vol. 9, no. 1, pp. 117–125, 2007.

[50] J. Steffens and J. R. Coury, “Collection efficiency of fiber filters operating on the removal of nano-sized aerosol particles: I—Homogeneous fibers” *Separation and Purification Technology*, vol. 58, no. 1, pp. 99–105, 2007.

[51] L. Boskovic, I. E. Agranovski, I. S. Altman, and R. D. Braddock, “Filter efficiency as a function of nanoparticle velocity and shape” *Journal of Aerosol Science*, vol. 39, no. 7, pp. 635–644, 2008.

[52] H.-L. Huang, D.-M. Wang, S.-T. Kao, S. Yang, and Y.-C. Huang, “Removal of monodisperse liquid aerosols by using the polysulfone membrane filters” *Separation and Purification Technology*, vol. 54, no. 1, pp. 96–103, 2007.

[53] G. A. Stevens and E. S. Moyer, “‘Worst case’ aerosol testing parameters: I. Sodium chloride and dioctyl phthalate aerosol filter efficiency as a function of particle size and flow rate” *American Industrial Hygiene Association Journal*, vol. 50, no. 5, pp. 257–264, 1989.

[54] B. Fardi and B. Y. Liu, “Performance of disposable respirators” *Particle and Particle Systems Characterization*, vol. 8, no. 1–4, pp. 308–314, 1991.

[55] C. C. Chen, M. Lehtimäki, and K. Willeke, “Aerosol penetration through filtering facepieces and respirator cartridges” *American Industrial Hygiene Association Journal*, vol. 53, no. 9, pp. 566–574, 1992.

[56] J. T. Hanley and K. K. Foarde, “Validation of Respirator Filter Efficacy” DTIC Document, 2003.

[57] H. S. Jordan and L. Silverman, “Effect of Pulsating Air Flow on Fiber Filter Efficiency” Harvard University, Boston. School of Public Health, 1961.

[58] R. G. Stafford, H. J. Ettinger, and T. J. Rowland, “Respirator cartridge filter efficiency under cyclic-and steady-flow conditions” *American Industrial Hygiene Association Journal*, vol. 34, no. 5, pp. 182–192, 1973.

[59] L. M. Brosseau, M. J. Ellenbecker, and J. S. Evans, “Collection of silica and asbestos aerosols by respirators at steady and cyclic flow” *American Industrial Hygiene Association Journal*, vol. 51, no. 8, pp. 420–426, 1990.

[60] A. W. Richardson, J. P. Eshbaugh, K. C. Hofacre, and P. D. Gardner, “Respirator filter efficiency testing against particulate and biological aerosols under moderate to high flow rates” Battelle Memorial Institute Columbus Ohio, US, 2006.

[61] H. Haruta, T. Honda, R. M. Eninger, T. Reponen, R. McKay, and S. A. Grinsphun, “Experimental and theoretical investigation of the performance of N95 respirator filters against ultrafine aerosol particles tested at constant and cyclic flows” *Journal of the International Society for Respiratory Protection*, vol. 25, pp. 75–88, 2008.

[62] K. J. Cho, T. Reponen, R. Mckay, R. Shukla, H. Haruta, P. Sekar, and S. A. Grinshpun, “Large particle penetration through N95 respirator filters and facepiece leaks with cyclic flow” *Annals of Occupational Hygiene*, vol. 54, no. 1, pp. 68–77, 2010.

[63] S. A. Grinshpun, H. Haruta, R. M. Eninger, T. Reponen, R. T. McKay, and S.-A. Lee, “Performance of an N95 filtering facepiece particulate respirator and a surgical mask during human breathing: Two pathways for particle penetration” *Journal of Occupational and Environmental Hygiene*, vol. 6, no. 10, pp. 593–603, 2009.

[64] J. P. Eshbaugh, P. D. Gardner, A. W. Richardson, and K. C. Hofacre, “N95 and P100 respirator filter efficiency under high constant and cyclic flow” *Journal of Occupational and Environmental Hygiene*, vol. 6, no. 1, pp. 52–61, 2009.

[65] S. Rengasamy and B. C. Eimer, “Total inward leakage of nanoparticles through filtering facepiece respirators” *Annals of Occupational Hygiene*, vol. 55, no. 3, pp. 253–263, 2011.

[66] A. Wang, A. W. Richardson, and K. C. Hofacre, “The Effect of Flow Pattern on Collection Efficiency of Respirator Filters” *Journal of the International Society for Respiratory Protection*, vol. 29, no. 1, pp. 41–54, 2012.

[67] X. He, M. Yermakov, T. Reponen, R. T. McKay, K. James, and S. A. Grinshpun, “Manikin-based performance evaluation of elastomeric respirators against combustion particles” *Journal of Occupational and Environmental Hygiene*, vol. 10, no. 4, pp. 203–212, 2013.

[68] X. He, S. A. Grinshpun, T. Reponen, M. Yermakov, R. McKay, H. Haruta, and K. Kimura, “Laboratory Evaluation of the Particle Size Effect on the Performance of an Elastomeric Half-mask Respirator against Ultrafine Combustion Particles” *Annals of Occupational Hygiene*, vol. 57, no. 7, pp. 884-897, 2013.

[69] P. D. Gardner, J. P. Eshbaugh, S. D. Harpest, A. W. Richardson, and K. C. Hofacre, “Viable Viral Efficiency of N95 and P100 Respirator Filters at Constant and Cyclic Flow” *Journal of Occupational and Environmental Hygiene*, vol. 10, no. 10, pp. 564–572, 2013.

[70] X. He, T. Reponen, R. T. McKay, and S. A. Grinshpun, “Effect of Particle Size on the Performance of an N95 Filtering Facepiece Respirator and a Surgical Mask at Various Breathing Conditions” *Journal of Aerosol Science*, vol. 47, no. 11, pp. 1180-1187, 2013.

[71] X. He, T. Reponen, R. T. McKay, and S. A. Grinshpun, “How Does Breathing Frequency Affect the Performance of an N95 Filtering Facepiece Respirator and a Surgical Mask Against Surrogates of Viral Particles?” *Journal of Occupational and Environmental Hygiene*, vol. 11, no. 3, pp. 178–185, 2013.

[72] X. He, S. A. Grinshpun, T. Reponen, R. McKay, M. S. Bergman, and Z. Zhuang “Effects of Breathing Frequency and Flow Rate on the Total Inward Leakage of an Elastomeric Half-Mask Donned on an Advanced Manikin Headform” *Annals of Occupational Hygiene*, vol. 58, no. 2, pp. 182-194, 2013.

73] S. P. Blackie, M. S. Fairbarn, N. G. McElvaney, P. G. Wilcox, N. J. Morrison, and R. L. Pardy, “Normal values and ranges for ventilation and breathing pattern at maximal exercise” *Chest Journal*, vol. 100, no. 1, pp. 136–142, 1991.

[74] D. M. Caretti, P. D. Gardner, and K. M. Coyne, "Workplace breathing rates: defining anticipated values and ranges for respirator certification testing" Defense Technical Information Center, 2004.

[75] L. L. Janssen, N. J. Anderson, P. E. Cassidy, R. A. Weber, and T. J. Nelson, "Interpretation of inhalation airflow measurements for respirator design and testing" *Journal of the International Society for Respiratory Protection*, vol. 22, no. 3/4, p. 122, 2005.

[76] N. J. Anderson, P. E. Cassidy, L. L. Janssen, and D. R. Dengel, "Peak Inspiratory Flows of Adults Exercising at Light, Moderate and Heavy Work Loads" *Journal of the International Society for Respiratory Protection*, vol. 23, no. 1/2, p. 53, 2006.

[77] W. W.-F. Leung and C.-H. Hung, "Investigation on pressure drop evolution of fibrous filter operating in aerodynamic slip regime under continuous loading of sub-micron aerosols" *Separation and Purification Technology*, vol. 63, no. 3, pp. 691–700, 2008.

[78] W. W.-F. Leung and C.-H. Hung, "Skin effect in nanofiber filtration of submicron aerosols" *Separation and Purification Technology*, vol. 92, pp. 174–180, 2012.

[79] L. W. Barrett and A. D. Rousseau, "Aerosol loading performance of electret filter media" *American Industrial Hygiene Association Journal*, vol. 59, no. 8, pp. 532–539, 1998.

[80] E. S. Moyer and M. S. Bergman, "Electrostatic N-95 respirator filter media efficiency degradation resulting from intermittent sodium chloride aerosol exposure" *Applied Occupational and Environmental Hygiene*, vol. 15, no. 8, pp. 600–608, 2000.

[81] A. Mahdavi, A. Bahloul, F. Haghighat, and C. Ostiguy, "Contribution of Breathing Frequency and Inhalation Flow Rate on Performance of N95 Filtering Facepiece Respirators" *Annals of Occupational Hygiene*, vol. 58, no. 2, pp. 195–205, 2014.

[82] R. Mostofi, A. Noël, F. Haghighat, A. Bahloul, J. Lara, and Y. Cloutier, "Impact of two particle measurement techniques on the determination of N95 class respirator filtration performance against ultrafine particles" *Journal of Hazardous Materials*, vol. 217, pp. 51–57, 2012.

[83] G. Berndtsson, "Peak Inhalation Air Flow and Minute Volumes Measured in a Bicycle Ergometer Test" *Journal of the International Society for Respiratory Protection*, vol. 21, no. 1–2, pp. 21–29, 2004.

[84] A. Bahloul, A. Mahdavi, F. Haghighat, and C. Ostiguy , "Evaluation of N95 filtering facepiece respirator efficiency with cyclic and constant flows" *Journal of Occupational and Environmental Hygiene*, vol. 11, no. 8, pp. 499-508, 2014.

[85] K. Ikezaki, K. Iritani, T. Nakamura, and T. Hori, "Effect of Charging State of Particles on Electrets" *Journal of Electrostatics*, vol. 35, pp. 41–46, 1995.

[86] B. Lowkis and E. Motyl, "Electret properties of polypropylene fabrics" *Journal of electrostatics*, vol. 51-52, pp. 232–238, 2001.